13. Carbon and Oxygen Isotopes of Cool-Water Bryozoans from the Great Australian Bight and Their Paleoenvironmental Significance[1]

Hideaki Machiyama,[2] Tsutomu Yamada,[3] Naotomo Kaneko,[4] Yasufumi Iryu,[3] Kei Odawara,[3] Ryuji Asami,[3] Hiroki Matsuda,[5] Shunsuke F. Mawatari,[6] Yvonne Bone,[7] and Noel P. James[8]

ABSTRACT

The carbon and oxygen isotopic compositions of selected bryozoan skeletons from upper Pleistocene bryozoan mounds in the Great Australian Bight (Ocean Drilling Program Leg 182; Holes 1129C, 1131A, and 1132B) were determined. Cyclostome bryozoans, *Idmidronea* spp. and *Nevianipora* sp., have low to intermediate magnesian calcite skeletons (1.5–10.0 and 0.9–6.4 molar percentage [mol%] $MgCO_3$, respectively), but a considerable number include marine cements. The cheilostome *Adeonellopsis* spp. are biminerallic, principally aragonite, with some high magnesian calcite (HMC) (6.6–12.1 mol% $MgCO_3$). The HMC fraction of *Adeonellopsis* has lower $\delta^{13}C$ and similar $\delta^{18}O$ values compared with the aragonite fraction. Reexamination of modern bryozoan isotopic composition shows that skeletons of *Adeonellopsis* spp. and *Nevianipora* sp. form close to oxygen isotopic equilibrium with their ambient water. Therefore, changes in glacial-interglacial oceanographic conditions are preserved in the oxygen isotopic profiles. The bryozoan oxygen isotopic profiles are correlated well with marine isotope Stages 1–8 in Holes 1129C and 1132B and to Stages 1–4(?) in Hole 1131A. The horizons of the bryozoan mounds that yield skeletons with heavier oxygen isotopic values can be correlated with isotope Stages 2, 4(?), 6, and

[2]Deep Sea Research Department, Japan Marine Science and Technology Center, 2-15 Natsushima-cho, Yokosuka 237-0061, Japan. **bucci@jamstec.go.jp**
[3]Institute of Geology and Paleontology, Graduate School of Science, Tohoku University, Aobayama, Sendai 980-8578, Japan.
[4]Geological Survey of Japan, AIST, 1-1-1 Higashi, Tsukuba 305-8567, Japan.
[5]Department of Earth Science, Kumamoto University, 2-39-1 Kurokami, Kumamoto 860-8555, Japan.
[6]Division of Biological Sciences, Graduate School of Science, Hokkaido University, N10 W8, Kita-ku, Sapporo 060-0810, Japan.
[7]Department of Geology and Geophysics, The University of Adelaide, SA 5005, Australia.
[8]Department of Geological Sciences, Queen's University, Kingston ON K7L 3N6, Canada.

8 in Hole 1129C; Stages 2 and 4(?) in Hole 1131A; and Stages 2, 4, 6, and 8 in Hole 1132B. These results provide supporting evidence for a model for bryozoan mound formation, in which the mounds were formed during intensified upwelling and increased trophic resources during glacial periods.

INTRODUCTION

Modern shelf carbonates are produced and deposited in tropical environments and in nontropical settings. Since Chave (1967) pointed out that carbonates could form at all latitudes, many investigations have been conducted on sedimentology of modern nontropical carbonates (Nelson, 1988; James, 1997). The comparative sedimentology showed that the carbonates produced in mid to high latitudes on high-energy open shelves may be good analogues for many ancient shelf limestones (James and Bone, 1989, 1991; James and von der Borch, 1991; James et al., 1992). These nontropical shelves have been the sites of extensive carbonate production and accumulation through the Phanerozoic.

The modern southern Australian continental margin constitutes the largest cool-water carbonate platform on Earth (Connolly and von der Borch, 1967; Wass et al., 1970; Marshall and Davies, 1978; Bone et al., 1992; James et al., 1992; Bone and James, 1993; Feary and James, 1995, 1998; James et al., 2001). The modern shelf sedimentation is controlled dominantly by swells and storms. The shelf is "shaved" under such a condition, with most skeletal fragments transported seaward to the shelf edge and slope or moved landward (James et al., 1994). The sediments consist exclusively of heterozoan skeletal constituents containing abundant bryozoans (cf. James, 1997).

Seismic images indicate that the platform, composed predominantly of successions of cool-water carbonate sediments, includes numerous biogenic buildups throughout the Cenozoic (Feary and James, 1995, 1998). Drilling into these structures revealed that they are bryozoan reef mounds constructed by a diverse suite of bryozoans (James et al., 2000). The bryozoan mounds were considered to have grown at paleowater depths of 80–200 m during glacial lowstands, when upwelling was intensified and consequently nutrient supply increased along the southern Australian continental margin (James et al., 2000). This nutrient-rich marine environment was caused by a combination of changes in oceanographic conditions during glacial periods (e.g., the subtropical convergence moved northward, there were strong offshore westerlies, and the Leeuwin Current weakened considerably or ceased flowing) (Wells and Wells, 1994; Wells and Okada, 1996; Okada and Wells, 1997).

Bryozoans are the principal constituents of deeper cool-water carbonates. In spite of this potential availability of bryozoan skeletons for paleoenvironmental reconstruction (Bone and James, 1997; Crowley and Taylor, 2000), the isotopic records have not been used for paleoceanographic determinations. This research aims to examine the downhole isotopic records of bryozoan skeletons collected from the Great Australian Bight (Ocean Drilling Program [ODP] Leg 182; Sites 1129, 1131, and 1132) and to discuss the late Pleistocene bryozoan mound developments. Also presented is an evaluation of the validity of bryozoan isotopic records as a paleoceanographic proxy.

GEOLOGIC SETTING

The Great Australian Bight is located on the central part of the southern continental margin of Australia. The Eucla Shelf, 1300 km in lateral extent and up to 260 km wide, is the site of the bryozoan mounds (Fig. F1). This divergent passive continental margin formed by the separation of the Australian continent from the Antarctica in the mid-Cretaceous and by the subsequent northward drift (Veevers et al., 1991). This continental margin has been a province of cool-water carbonate deposition since Eocene time, overlying Mesozoic basal siliciclastic sequences (McGowran et al., 1997; Feary and James, 1998; Feary, Hine, Malone, et al., 2000). The shelf edge to upper slope of the Eucla Shelf is marked by a huge sediment wedge, consisting of prograding clinoforms of entirely Quaternary age (cf. Feary and James, 1998; Feary, Hine, Malone, et al., 2000), so the shelf margin resembles a distally steepened ramp (cf. Read, 1985). This sediment wedge is >500 m thick, giving an accumulation rate exceeding 40 cm/k.y. (Hine et al., 1999). This is equivalent to the rate of modern shallow-water tropical carbonates and twice as high as the rate of modern slope deposition on the Bahama Banks (cf. Eberli, Swart, Malone, et al., 1997).

Bryozoan reef mounds were drilled at Sites 1129, 1131, and 1132 at modern water depths of 200–350 m, which coincide with the facies transition zone from shallower coarse-grained bryozoan-rich shelf sediments to deeper fine-grained spiculitic mud (James et al., 1994, 2001). Seismic images indicate that these mounds have a depositional relief of ~50 m or more and markedly elongate features, extending to several kilometers parallel to the slope and to several hundred of meters normal to the slope (Feary and James, 1995, 1998; Feary, Hine, Malone, et al., 2000; James et al., 2000). They occur both as isolated mounds and as mound complexes that grade laterally into surrounding evenly bedded sediments. Drilling into these mounds has shown that the mounds have an unlithified floatstone to rudstone texture and are constructed primarily of a diverse suite of up to pebble-sized bryozoans (Feary, Hine, Malone, et al., 2000; James et al., 2000). All bryozoan growth forms are present in varying degrees (cf. Bone and James, 1993). The poorly sorted muddy "matrix" consists mainly of benthic and planktonic foraminifers, fecal pellets, singlets of articulated zooidal bryozoans, sponge and tunicate spicules, and calcareous nannofossils with a lime mudstone to packstone texture.

In this study, we determined the stable isotopic values of bryozoan skeletons collected from the upper parts of Holes 1129C, 1131A, and 1132B, in which the bryozoan reef mounds were situated. Site 1129 at 202 mean water depth (mwd) is located slightly down the shelf slope (Fig. F1) and includes bryozoan mound complexes in the upper 150 m of the Pleistocene succession. The upper 150 m of Hole 1129C consists mainly of bryozoan floatstone to rudstone and bioclastic packstone to grainstone, with abundant bryozoan fragments (Feary, Hine, Malone, et al., 2000) (Fig. F2). Unlithified boundstones form thick intervals (up to 10 m thick) from 41 to 62.5 meters below seafloor (mbsf) and from 72.3 to 86.3 mbsf and are also found as thin intervals (<1 m thick) from 5.9 to 19.3 mbsf and from 132.9 to 142.6 mbsf (Fig. F2). Several packets, each of which begins with basal bioclastic packstone and/or wackestone that grade upward into bryozoan boundstone, are found in this hole (Feary, Hine, Malone, et al., 2000). These single packets are ~18–41 m in thickness. Site 1131, at 332 mwd, is situated off Site 1129 on the upper

F1. Map showing the location of ODP Leg 182 sites in the Great Australian Bight, p. 14.
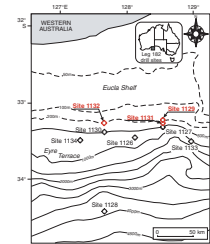
F2. $\delta^{13}C_{corr}$ and $\delta^{18}O_{corr}$ profiles of three genera of bryozoans, Hole 1129C, p. 15.
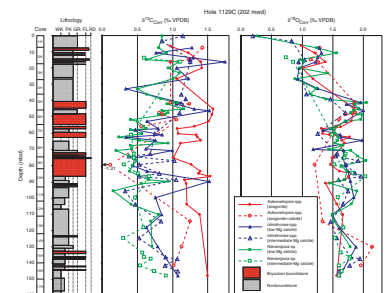
slope (Fig. F1) and contains bryozoan mound complexes in the upper-most part of the Pleistocene succession (Feary, Hine, Malone, et al., 2000; James et al., 2000). The upper 40 m of Hole 1131A consists mainly of bryozoan floatstone to rudstone and massive homogeneous bioclastic packstone with a wackestone layer (Feary, Hine, Malone, et al., 2000) (Fig. F3). Some intervals (up to 4.8 m thick) of unlithified boundstones are present from 4.8 to 24.8 mbsf (Fig. F3). Site 1132, at 218 mwd, is immediately seaward of the shelf (Fig. F1). The upper 135 m of Hole 1132B chiefly comprises bryozoan floatstone to rudstone and bioclastic packstone to wackestone with abundant bryozoan fragments (Feary, Hine, Malone, et al., 2000) (Fig. F4). Unlithified boundstones are present, forming many thick intervals (up to 5 m thick) associated with some thin layers (decimeter scale), corresponding to major bryozoan mound complexes in the upper 90 m of the Pleistocene succession (Feary, Hine, Malone, et al., 2000).

MATERIAL AND METHODS

Samples

A total of 407 samples from Holes 1129C, 1131A, and 1132B were examined in this study (Table T1). These samples contained common to abundant bryozoan skeletons. More than 60 genera were present. About 80% of the genera were assigned to cheilostomes. Although the cyclostomes were not so diverse, they were volumetrically important constituents. The bryozoan fauna was dominated by delicate branching cyclostomes and flat robust branching, articulated branching, and fenestrate cheilostomes. Large fragments of nodular/arborescent cheilostomes were rare but, when present, comprised >50% of the total bryozoan skeletal weight. Articulated branching cyclostomes and articulated zooidal cheilostomes were found in most samples, but they were minor components. The dominant genera included *Adeonellopsis, Cellaria, Phidoloporidae* gen. indet., *Nevianipora, Idmidronea, Hornera,* and *Crisia.* Surface features of the bryozoan skeletons were well preserved, although the zoaria were broken and fragmented. Some skeletons were abraded and/or cemented.

We studied three genera of bryozoans (*Idmidronea* spp., *Nevianipora* sp., and *Adeonellopsis* spp.) because they were abundant in many samples (Fig. F5). Their characteristic features were as follows:

Nevianipora sp. is a delicate branching cyclostome, the colonies are branched dichotomously, the transverse shape of the branch is oval with flattened back, the autozooid opening is limited to one side of the branch, and peristomes are projected alternately (Fig. F5A).
Idmidronea spp. are also a delicate branching cyclostomes but differ from *Nevianipora* sp. by forming more delicate and fragile colonies (Fig. F5B).
Adeonellopsis spp. are flat robust branching cheilostome. Their colonies are more robust than the other genera (Fig. F5C).

F3. $\delta^{13}C_{corr}$ and $\delta^{18}O_{corr}$ profiles of three genera of bryozoans, Hole 1131A, p. 16.
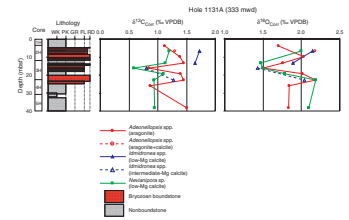
F4. $\delta^{13}C_{corr}$ and $\delta^{18}O_{corr}$ profiles of three genera of bryozoans, Hole 1132B, p. 17.
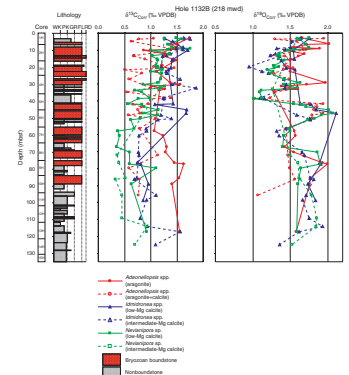
T1. Isotopic composition and carbonate mineralogy of bryozoans, Holes 1129C, 1131A, and 1132B, p. 23.

F5. Scanning electron photomicrographs of the bryozoans examined in this study, p. 18.
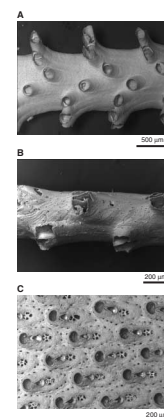
ANALYTICAL METHODS

All samples were washed with water over a 0.5-mm mesh sieve to remove the mud fraction, then dried in an oven at 25°C. Fragments of bryozoan skeletons in a good state of preservation were selectively picked under a binocular microscope. Before mineralogical and isotopic analyses, the skeletons were broken into several pieces and the fine carbonate fractions were removed under a binocular microscope. Several skeletons were observed with a field emission scanning electron microscope (SEM) (JEOL JSM-6330F) or with a low-vacuum SEM (JEOL JSM-5800LV) to check whether the material had been diagenetically altered. Although a small amount of carbonate cement was observed in the skeletons collected at depths >40 mbsf (Fig. F6), further pretreatment to remove cements such as hydrogen peroxide soaking (Sakai and Kano, 2001) was not carried out because our preliminary analysis indicates that the H_2O_2 treatment affected the isotopes. All samples were powdered prior to mineralogical analyses.

Mineralogy and molar percentage (mol%) $MgCO_3$ of bryozoan of skeletal carbonate were determined by X-ray diffraction (XRD) using a Philips X'pert-MPD (PW3050) with CuK_α radiation and a Ni filter. Samples (~0.5–1.0 mg) were ground to fine particles (~10 μm in diameter) by careful grinding by hand. A smear mount was prepared by smearing the particles with distilled water on to a silicon plate (nonreflection) and then air dried. The goniometer scanned from 20° to 40°2θ with a step size of 0.02°2θ and a count time of 2.0 s/step for all samples. A tube voltage of 40 kV and a tube current of 55 mA were used. Diffractograms were stripped to remove $K_{\alpha 2}$ signal and smoothed. Mineral weight percentages were calculated by the integrated peak intensity procedures following Cook et al. (1975). Magnesium content in skeletal carbonate was determined by displacement of the d_{104} peak of calcite with increasing $MgCO_3$ (Goldsmith and Graf, 1958). Precision of XRD through the whole experiment was estimated by measuring the positions of the d_{111} and d_{220} peaks of silicon before and after a sequences of daily analyses (15–20 samples) and was less than ±0.01°2θ. This implies that concentrations determined by XRD are accurate to ±0.3 mol% $MgCO_3$.

The skeletons were processed by an automated carbonate device (Kiel III, Finnigan MAT GmbH) attached to a Finnigan MAT Delta S mass spectrometer at the Institute of Geology and Paleontology, Graduate School of Science, Tohoku University, or by the same device attached to a Finnigan MAT 252 mass spectrometer at the Technological Research Center, Japan National Oil Corporation (TRC/JNOC). A sample of ~0.1 mg was separately dissolved to CO_2 by "105%" phosphoric acid in a vacuum at 70°C (at Tohoku University) or at 72°C (at TRC/JNOC) in a reaction vessel. The results of isotope analysis were corrected for the usual isobaric interferences using the equations of Santrock et al. (1985) and presented according to the conventional notation in parts per thousand deviation from the international standard, Vienna Peedee belemnite (VPDB). After correction for the difference in oxygen isotopic fractionation between reaction temperatures of 25°, 70°, and 72°C, $\delta^{18}O$ of carbonate sample was calculated using $\alpha = 1.01025$ at 25°C for calcite (Sharma and Clayton, 1965; Friedman and O'Neil, 1977) and $\alpha = 1.01034$ at 25°C for aragonite (Sharma and Clayton, 1965; Friedman and O'Neil, 1977). The conversion between VPDB and Vienna Standard Mean Ocean Water (VSMOW) scales was calculated using the equations of Coplen et al. (1983). External precision through the whole experi-

F6. Scanning electron photomicrographs of skeletons of *Nevianipora* sp., Hole 1129C, p. 19
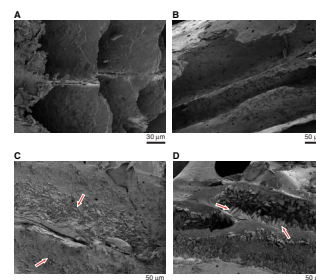
ment was estimated from four to eight analyses of internal laboratory calcite standard (MACS1) inserted in every batch of samples (20–44 samples) and was $<\pm0.05$‰ for $\delta^{13}C$ and ±0.08‰ for $\delta^{18}O$ (±1 σ, $N = 72$). Several measurements of the internal laboratory standards showed that differences in isotopic compositions of the same material between two laboratories was negligibly small (<0.1‰ for $\delta^{13}C$ and $\delta^{18}O$).

RESULTS

Mineralogy

XRD measurements indicate that *Idmidronea* spp. and *Nevianipora* sp. have calcite skeletons with 1.5–10.0 and 0.9–6.4 mol% $MgCO_3$, respectively (Table T1). These bryozoans fall into the low magnesian calcite (LMC) (mol% $MgCO_3$) and the intermediate magnesian calcite (IMC) (4–12 mol% $MgCO_3$) mineralogical groupings of Bone and James (1993). SEM observations, however, indicate that the bryozoan skeletons have been subject to variable marine diagenesis below the flushed zones (Fig. F6). Therefore, the above values do not totally represent the original skeletal mineralogy, possibly with lower magnesian contents. *Adeonellopsis* spp. have an aragonite skeleton accompanied by significant amounts (up to 59%) of IMC (Table T1). The volume of calcite varies from stratigraphic horizon to horizon and from sample to sample even within the same horizon.

Stable Isotopic Composition

Bryozoan carbon and oxygen isotopic profiles for Holes 1129C, 1131A, and 1132B are shown in Figures F2, F3, and F4, respectively. In these depth profiles, we used the average value of the same groups collected from the same depth. The groups include the LMC and IMC mineralogical groups of *Idmidronea* spp. and *Nevianipora* sp. and aragonite and aragonite + calcite groups of *Adeonellopsis* spp. It can be considered that the LMC groups of *Idmidronea* and *Nevianipora* and aragonitic *Adeonellopsis* may have less marine cements and retain more original isotopic signals than the rests. A sharp negative shift of $\delta^{18}O$ values is discernible at ~40 mbsf in Hole 1129C, above which the profiles are characterized by relatively lighter values and larger amplitudes (up to 1.3‰). *Idmidronea* spp. and *Nevianipora* sp. show the lightest oxygen isotopic values of ~0.2‰ and 0.3‰ at the top of Hole 1129C, which consists of a thin Holocene sediment veneer. In contrast, the isotopic values are heavier, and the profiles have smaller amplitudes (<1.0‰) at 40 mbsf downhole. This negative shift is not clearly recognized in Holes 1131A or 1132B.

DISCUSSION

Isotopic Composition of Modern Bryozoans

Isotopic composition of living and dead bryozoan skeletons has been measured by several studies. Bone and James (1997) noted the isotopic composition of *Adeonellopsis* and *Nevianipora* from the Lacepede Shelf, east of our study area. We evaluate reliability of the bryozoan isotopes as a proxy for their inhabiting environment by examining their data.

Bone and James (1997) reported summer and winter temperature profiles of water column and isotopic composition of surface water on the Lacepede Shelf but did not give any data on salinity. According to oceanographic data from LEVITUS94 (Levitus et al., 1994; Levitus and Boyer, 1994), spatial differences in mean annual salinity and mean annual temperatures of surface water are negligibly small (~0.15° and 0.4°C, respectively) at the sites where Bone and James (1997) collected *Adeonellopsis* and *Nevianipora*. Salinity and temperatures decrease uniformly with depth at those sites.

We calculated the equilibrium field of $\delta^{18}O$ values for pure calcite and aragonite precipitated in isotopic oxygen equilibrium with bryozoan's ambient seawater, using the following method.

1. $\delta^{18}O$ of surface water is presumed to be 0‰ VSMOW.
2. $\delta^{18}O$ values of bottom water are estimated using the salinity profiles and relationships between changes in $\delta^{18}O$ of water and those in salinity ($\Delta\delta^{18}O_W/\Delta\delta = 0.50$) (Broecker, 1989).

Then, $\delta^{18}O$ of equilibrium pure calcite was estimated by an equation of Friedman and O'Neil (1977) using temperature data from LEVITUS94. All of our isotopic values were corrected ($\delta^{18}O_{corr}$ and $\delta^{13}C_{corr}$) for the following fractionations:

Aragonite is enriched in $\delta^{18}O$ by 0.6‰ compared to calcite precipitated under the same conditions (Tarutani et al., 1969). The $\delta^{18}O$ in magnesian calcite is higher relative to pure calcite by 0.06‰ for each mol% $MgCO_3$ in the calcite (Tarutani et al., 1969). Aragonite is enriched in $\delta^{13}C$ by 1.7‰ compared to coprecipitated calcite (Romanek et al., 1992).

It is clearly shown that *Adeonellopsis* and *Nevianipora* precipitate their skeleton nearly in oxygen isotopic equilibrium with ambient seawater (Fig. F7). Consequently, it is plainly evident that $\delta^{18}O$ of these bryozoans is a useful proxy as oceanographic conditions where the bryozoans grew.

Carbon isotopic composition of the equilibrium calcite and aragonite is not calculated because little is known on $\delta^{13}C$ of dissolved inorganic carbon of bottom water in the Lacepede Shelf.

Diagenetic Influence on Bryozoan Isotopes

If diagenesis has occurred, then the isotopic composition of the bryozoans from Holes 1129C, 1131A, and 1132B will have been changed as a result of this diagenetic alteration. A profile of chemical properties, such as Sr concentrations in interstitial water from Site 1129, indicates that the properties are rather homogenous and similar to those of ambient seawater in the interval of 0–40.3 mbsf. Consequently, this interval is thought of as a flushed zone. Sediments within this zone contain a large volume of HMC and aragonite but no dolomite (Feary, Hine, Malone, et al., 2000). Below this zone, HMC and aragonite are less common, and instead, LMC is more abundant. Bryozoans collected from 0.40 mbsf are thought to retain their original isotopic composition because their $\delta^{18}O$ and $\delta^{13}C$ values are close to those of pure calcite that is precipitated in isotopic equilibrium with ambient seawater with

$$\delta^{18}O_{H_2O} = -0.2‰$$

F7. Comparisons of $\delta^{18}O$ pure calcite and aragonite and *Adeonellopsis* and *Nevianipora,* p. 20.
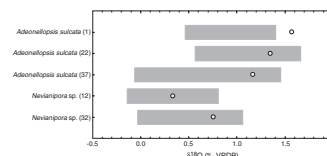
(calculated from salinity from LEVITUS94 data and $\delta^{18}O_{H_2O}$ values of surface water [Bone and James, 1997]) at 13.4° (mean annual temperature of bottom water [LEVITUS94 data]). Thus, bryozoan skeletons in the flushed zone may retain their original isotopic composition. Below the flushed zone, the sediments have been variably subjected to diagenesis. This conclusion is supported by two lines of evidence:

1. The degree of cementation observed with SEM and
2. Carbonate mineralogy (more dissolution = higher Sr^{2+} concentration in the interstitial water, more LMC, and less HMC and aragonite below the flushed zone) (Feary, Hine, Malone, et al., 2000).

Few diagenetic signatures were observed in the uppermost 10 m of sediments in Hole 1131A, below which the sediments have been diagenetically altered to varying degrees. The flushed zone is also recognized in Hole 1132B, where the sediments in the interval 0–30.3 mbsf have been hardly subjected to diagenesis.

In this study, we investigated relationships between the mineralogy and isotopic composition of *Adeonellopsis.* The mineralogy is highly variable from specimen to specimen. Some skeletons consist exclusively of aragonite, and others are associated with IMC (6.6–12.1 mol% $MgCO_3$). There is no regular relationship between mineralogy (calcite content) and $\delta^{18}O$ (Fig. F8A). It is worthwhile to note that the $\delta^{18}O$ values range widely even if the skeletal mineralogy is similar. In the case of the skeletons consisting of pure aragonite, the $\delta^{18}O$ values range from 1.43‰ to 2.79‰, with a standard deviation (1σ) of 0.27 (mean = 2.17‰; N = 89). In contrast, the $\delta^{13}C$ values decrease with increasing calcite content (Fig. F8B). These data indicate that the original aragonitic skeletons may be accompanied by calcites that have smaller $\delta^{13}C$ and similar $\delta^{18}O$ values compared with the aragonite. Possible explanations include secondary thickening and/or diagenetic alterations.

Bryozoan Isotopic Profiles

Bryozoan oxygen isotopic profiles in Holes 1129C, 1131A, and 1132B are compared with the standard Quaternary oxygen isotopic record (Berger et al., 1994) (Fig. F9). Oxygen isotopic profiles of the three genera are generally similar to each other with some outliers. We referred to accelerator mass spectrometer (AMS) ^{14}C and U-series ages (N.P. James et al., unpubl. data) to match the curves. The oxygen isotope profiles of Holes 1129C and 1132B can be correlated with marine isotope Stages 1–8 and those of Hole 1131A to Stages 1–4(?). Paucity of bryozoans below ~90 mbsf does not allow precise correlation with stages older than isotope Stage 9 in Holes 1129C and 1132B. It also seems that Stages 3 and 5 are not clearly discriminated in the isotopic profiles from Hole 1129C nor is Stage 2 in Hole 1132B.

Amplitudes of the profiles from Hole 1129C are smaller (<1‰) than those of the standard Quaternary oxygen isotopic record (<1.5‰), except for the large shifts at ~0–10 and 40 mbsf. Possible explanations for these include the following:

1. Differences in temperatures between glacial and interglacial periods are much less in the Great Australian Bight than those re-

F8. Relationships between carbonate mineralogy and isotopic composition of *Adeonellopsis,* p. 21.
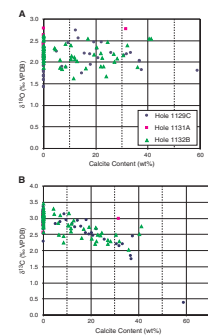
F9. Correlation of bryozoan oxygen isotopic profiles and Quaternary oxygen isotopic record, p. 22.
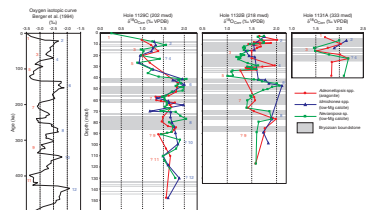
corded in planktonic foraminifers from the Ontong Java (Berger et al. 1994).

2. The original differences in isotopic signals between glacial and interglacial periods have been muted by diagenetic alterations.

Our observations indicate that the sediments below 40 mbsf have been variably subjected to diagenesis. Thus, the latter explanation (2) is acceptable. Even though diagenesis has caused significant shifts of original bryozoan isotopic profiles and reduction of the amplitude, the shape of the profiles may be preserved, although this suggestion cannot be substantiated

Overall the bryozoan mounds correspond well to the intervals that yield bryozoans with heavier oxygen isotopic values. These intervals are correlated with marine isotope Stages 2, 4(?), 6, and 8 in Hole 1129C, Stages 2 and 4(?) in Hole 1131A, and Stages 2, 4, 6, and 8 in Hole 1132B. In contrast, bryozoan mounds did not flourish during interglacial stages, especially isotope Stages 1 and 5, as observed in Holes 1129C and 1132B. James et al. (2000) proposed a model for the mound formation at Site 1131 during the last glacial maximum. The mounds were formed by intensified upwelling and increased nutrient levels and trophic resources during glacial periods when the Leeuwin Current, which carries warm nutrient-depleted low-salinity water that forms a zone ~50 km wide and 200 m deep from off western Australia around Cape Leeuwin into the Great Australian Bight, was inactive (e.g., Wells and Wells, 1994; Wells and Okada, 1996; McGowran et al., 1997; Okada and Wells, 1997; James et al., 1999). Our data provide supporting evidence for this model.

Although *Adeonellopsis* spp., *Idmidronea* spp., and *Nevianipora* sp. have similar $\delta^{18}O_{corr}$ values, the $\delta^{13}C_{corr}$ values are quite different from one another. *Nevianipora* sp. has slightly lighter $\delta^{13}C$ values than *Idmidronea* spp. On the other hand, *Adeonellopsis* spp. has slightly heavier $\delta^{13}C$ values than *Idmidronea* spp. in Holes 1129C and 1131A, but no regular relationship is found in Hole 1132B. Figures F2, F3, and F4 show that carbon isotope fluctuation may not be related directly to glacial-interglacial oceanographic changes. Crowley and Taylor (2000) studied modern bryozoans collected from Otago Shelf, New Zealand, and showed that differences between the carbon isotopic composition of bryozoan skeletons from the same species and coexisting species living in the same community may be assignable to significant variations in the extent to which marine dissolved inorganic carbon (DIC) and respiratory CO_2 are utilized during calcification. Consequently, it seems very difficult to interpret the $\delta^{13}C$ signals in Holes 1129C, 1131A, and 1132B at this time.

CONCLUSIONS

Oxygen stable isotopic values of bryozoans from the upper Pleistocene sediments in the Great Australian Bight (ODP Leg 182, Holes 1129C, 1131A, and 1132B) suggest that the oxygen isotope signals can be potentially useful as a paleoceanographic proxy, providing they have not been diagenetically altered. However, in our study, the bryozoan $\delta^{18}O$ signals are not as sensitive as those of planktonic and benthic foraminifers.

This study led to the following conclusions:

The cyclostomes *Idmidronea* spp. and *Nevianipora* sp. have skeletons with LMC to IMC (1.5–10.0 and 0.9–6.4 mol% $MgCO_3$, respectively), but some skeletons may be enriched in Mg because of marine diagenesis (i.e., early marine cement). The cheilostome *Adeonellopsis* spp. have a mainly aragonitic skeleton, although some specimens have associated IMC (6.6 to 12.1 mol% $MgCO_3$). The latter have lower $\delta^{13}C$ and similar $\delta^{18}O$ values compared with the totally aragonitic specimens. Marine cements occur more frequently within intraskeletal spaces with increasing depth (>40 mbsf).

Reexamination of modern bryozoan data shows that (1) *Adeonellopsis* and *Nevianipora* form their skeletons at close to oxygen isotopic equilibrium with ambient seawater and (2) in contrast, the carbon isotopic composition reflects vital effects.

Glacial-interglacial cycles are detected from the oxygen isotope profiles. The profiles can be correlated with isotope Stages 1–8 in Holes 1129C and 1132B and with Stages 1–4(?) in Hole 1131A.

The bryozoan mounds generally coincide with heavier oxygen isotopic values during isotope Stages 2, 4(?), 6, and 8 in Hole 1129C, Stages 2 and 4(?) in Hole 1131A, and Stages 2, 4, 6, and 8 in Hole 1132B. Our results support a model in which the mounds were formed by intensified upwelling and increased nutrient levels and trophic resources during glacial periods when the warm nutrient-depleted Leeuwin Current was inactive.

ACKNOWLEDGMENTS

REFERENCES

Berger, W.H., Yasuda, M.K., Bickert, T., Wefer, G., and Takayama, T., 1994. Quaternary time scale for the Ontong Java Plateau: Milankovitch template for Ocean Drilling Program Site 806. *Geology,* 22:463–467.

Bone, Y., and James, N.P., 1993. Bryozoans as carbonate sediment producers on the cool-water Lacepede Shelf, Southern Australia. *Sediment. Geol.,* 86:247–271.

————, 1997. Bryozoan stable isotope survey from the cool-water Lacepede Shelf, southern Australia. *In* James, N.P. and Clarke, J.A.D., (Eds.) *Cool-Water Carbonates.* Spec. Pub.—SEPM (Soc. Sediment. Geol.), 56:93–105.

Bone, Y., James, N.P., and Kyser, T.K., 1992. Syn-sedimentary detrital dolomite in Quaternary cool-water carbonate sediments, Lacepede Shelf, south Australia. *Geology,* 20:109–112.

Broecker, W.S., 1989. The salinity contrast between the Atlantic and Pacific Oceans during glacial time. *Paleoceanography,* 4:207–212.

Chave, K.E., 1967. Recent carbonate sediments–an unconventional view. *J. Geol. Educ.,* 15:200–204.

Cook, H.E., Johnson, P.D., Matti, J.C., and Zemmels, I., 1975. Methods of sample preparation and X-ray diffraction data analysis, X-ray Mineralogy Laboratory, Deep Sea Drilling Project, University of California, Riverside. *In* Hayes, D.E., Frakes, L.A., et al., *Init. Repts. DSDP,* 28: Washington (U.S. Govt. Printing Office), 999–1007.

Connolly, J.R., and von der Borch, C.C., 1967. Sedimentation and physiography of the seafloor south of Australia. *Sediment. Geol.,* 1:181–220.

Coplen, T.B., Kendall, C., and Hopple, J., 1983. Comparison of stable isotope reference samples. *Nature,* 302:236–238.

Crowley, S.F., and Taylor, P.D., 2000. Stable isotope composition of modern bryozoan skeletal carbonate from the Otago Shelf, New Zealand. *N. Z. J. Mar. Freshwater Res.,* 34:331–351.

Eberli, G.P., Swart, P.K., Malone, M.J., et al., 1997. *Proc. ODP, Init. Repts.,* 166: College Station, TX (Ocean Drilling Program).

Feary, D.A., Hine, A.C., Malone, M.J., et al., 2000. *Proc. ODP, Init. Repts.,* 182 [CD-ROM]. Available from: Ocean Drilling Program, Texas A&M University, College Station, TX 77845-9547, U.S.A.

Feary, D.A., and James, N.P., 1995. Cenozoic biogenic mounds and buried Miocene (?) barrier reef on a predominantly cool-water carbonate continental margin, Eucla Basin, western Great Australian Bight. *Geology,* 23:427–430.

————, 1998. Seismic stratigraphy and geological evolution of the Cenozoic, cool-water Eucla Platform, Great Australian Bight. *AAPG Bull.,* 82:792–816.

Friedman, I., and O'Neil, J.R., 1977. Compilation of stable isotope fractionation factors of geochemical interest. *In* Fleischer, M. (Ed.), *Data of Geochemistry* (6th ed.). Geol. Surv. Prof. Pap. U.S., 440-KK:1–12.

Goldsmith, J.R., and Graf, D.L., 1958. Relations between lattice constraints and composition of the Ca-Mg carbonates. *Am. Mineral.,* 43:84–101.

Hine, A.C., Feary, D.A., Malone, M.J., Andres, M., Betzler, C., Brooks, G.R., Brunner, C.A., Fuller, M.D., Holbourn, A.E., Huuse, M., Isern, A.R., James, N.P., Ladner, B.C., Li, Q., Machiyama, H., Mallinson, D.J., Matsuda, H., Mitterer, R.M., Molina, G.R.S., Robin, C., Russell, J.L., Shafik, S., Simo, J.A.T., Smart, P.L., Spence, G.H., Surlyk, F., Swart, P.K., and Wortmann, U.G., 1999. Research in the Great Australian Bight yields exciting early results. *Eos,* 80:521–526.

James, N.P., 1997. The cool-water carbonate depositional realm. *In* James, N.P., and Clarke, J.A.D. (Eds.), *Cool-Water Carbonates.* Spec. Publ.—SEPM (Soc. Sediment. Geol.), 56:1–20.

James, N.P., and Bone, Y., 1989. Petrogenesis of Cenozoic temperate water calcarenites south Australia: a model for meteoric/shallow burial diagenesis of shallow water calcite sediments. *J. Sediment. Petrol.,* 59:191–203.

————, 1991. Origin of a cool-water, Oligo-Miocene deep shelf limestone, Eucla Platform, southern Australia. *Sedimentology,* 38:323–341.

James, N.P., Bone, Y., Collins, L.B., and Kyser, T.K., 2001. Surficial sediments of the Great Australian Bight: facies dynamics and oceanography on a vast cool-water carbonate shelf. *J. Sediment. Res.,* 71:549–567.

James, N.P., Bone, Y., von der Borch, C.C., and Gostin, V.A., 1992. Modern carbonate and terrigenous clastic sediments on a cool-water, high-energy, mid-latitude shelf: Lacepede, southern Australia. *Sedimentology,* 39:877–903.

James, N.P., Boreen, T.D., Bone, Y., and Feary, D.A., 1994. Holocene carbonate sedimentation on the west Eucla Shelf, Great Australian Bight: a shaved shelf. *Sediment. Geol.,* 90:161–177.

James, N.P., Collins, L.B., Bone, Y., and Hallock, P., 1999. Subtropical carbonates in a temperate realm: modern sediments on the southwest Australian shelf. *J. Sediment. Res.,* 69:1297–1321.

James, N.P., Feary, D.A., Surlyk, F., Simo, J.A., Betzler, C., Holbourn, A.E., Li, Q., Matsuda, H., Machiyama, H., Brooks, G.R., Andres, M.S., Hine, A.C., Malone, M.J., and the ODP Leg 182 Science Party, 2000. Quaternary bryozoan reef mounds in cool-water, upper slope environments, Great Australian Bight. *Geology,* 28:647–650.

James, N.P., and von der Borch, C.C., 1991. Carbonate shelf edge off southern Australia: a prograding open-platform margin. *Geology,* 19:1005–1008.

Levitus, S., and Boyer, T.P., 1994. *World Ocean Atlas 1994* (Vol. 4): *Temperature.* NOAA Atlas NESDIS 4.

Levitus, S., Burgett, R., and Boyer, T.P., 1994. *World Ocean Atlas 1994* (Vol. 3): *Temperature.* NOAA Atlas NESDIS 3.

Marshall, J.F., and Davies, P.J., 1978. Skeletal carbonate variations on the continental shelf of eastern Australia. *BMR J. Aust. Geol. Geophys.,* 3:85–92.

McGowran, B., Li, Q., and Moss, G., 1997. The Cenozoic neritic record in southern Australia: the biogeohistorical framework. *In* James, N.P., and Clarke, J., *Cool-Water Carbonates.* Spec. Publ.— SEPM (Soc. Sediment. Geol.), 56:185–203.

Nelson, C.S., 1988. An introductory perspective on non-tropical shelf carbonates. *Sediment. Geol.,* 60:3–12.

Okada, H., and Wells, P., 1997. Late Quaternary nannofossil indicators of climate change in two deep-sea cores associated with the Leeuwin Current off Western Australia. *Palaeogeogr., Palaeoclimatol., Palaeoecol.,* 131:413–432.

Read, J.F., 1985. Carbonate platform facies models. *AAPG Bull.,* 69:1–21.

Romanek, C.S., Grossman, E.T., and Morse, J.W., 1992. Carbonate isotope fractionation in synthetic aragonite and calcite: effects of temperature and precipitation rate. *Geochim. Comochim. Acta,* 56:419–430.

Sakai, S., and Kano, A., 2001. Original oxygen isotopic composition of planktonic foraminifers preserved in diagenetically altered Pleistocene shallow-marine carbonates. *Mar. Geol.,* 172:197–204.

Santrock, J., Studley, S.A., and Hayes, J.M., 1985. Isotopic analysis based on the mass spectrum of carbon dioxide. *Anal. Chem.,* 57:1444–1448.

Sharma, T., and Clayton, R.N., 1965. Measurement of $^{18}O/^{16}O$ ratios of total oxygen in carbonates. *Geochim. Cosmochim. Acta,* 29:1347–1353.

Tarutani, T., Clayton, R.N., and Mayeda, T.K., 1969. The effect of polymorphism and magnesium substitution on oxygen isotope fractionation between calcium carbonate and water. *Geochim. Cosmochim. Acta,* 33:987–996.

Veevers, J.J., Powell, C. McA., and Roots, S.R., 1991. Review of seafloor spreading around Australia, 1. Synthesis of patterns of spreading. *Aust. J. Earth Sci.,* 38:373–390.

Wass, R.E., Connolly, J.R., and Macintyre, J., 1970. Bryozoan carbonate sand continuous along southern Australia. *Mar. Geol.,* 9:63–73.

Wells, P., and Okada, H., 1996. Holocene and Pleistocene glacial palaeoceanography off southeastern Australia, based on foraminifers and nannofossils in Vema cored hole V18-222. *Aust. J. Earth Sci.,* 43:509–523.

Wells, P.E., and Wells, G.M., 1994. Large-scale reorganization of ocean currents offshore western Australia during the late Quaternary. *Mar. Micropaleontol.,* 24:157–186.

Figure F1. Map showing the location of ODP Leg 182 sites in the Great Australian Bight. Samples examined in this study were collected from Sites 1129, 1131, and 1132.
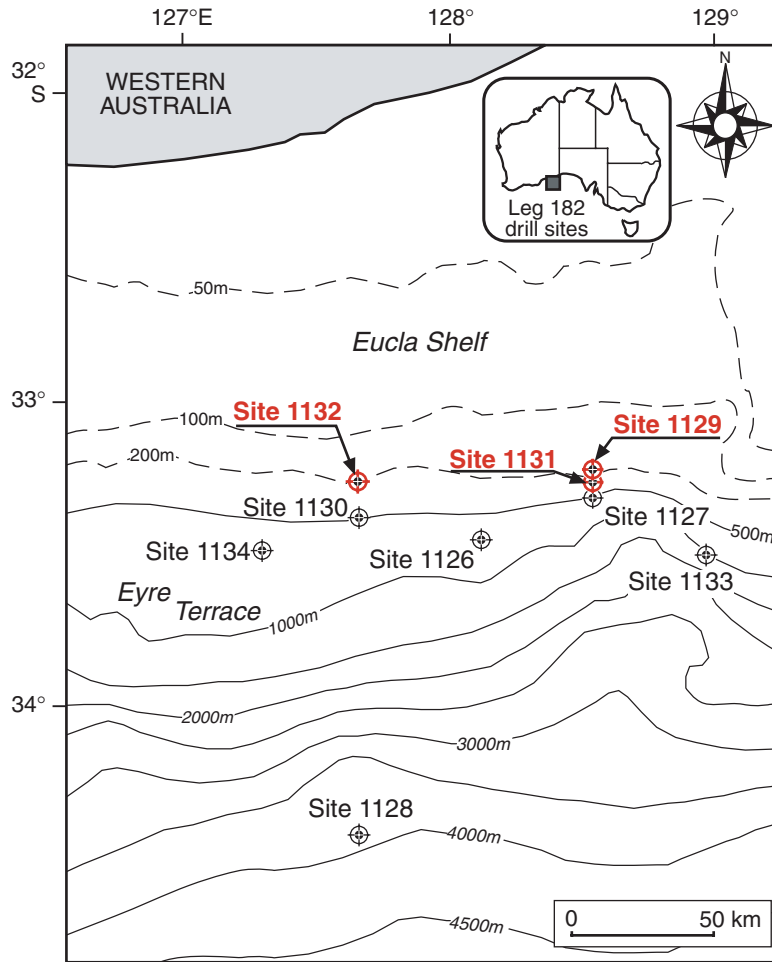
Figure F2. $\delta^{13}C_{corr}$ and $\delta^{18}O_{corr}$ profiles of three genera of bryozoans and simplified lithologic column of Hole 1129C. mwd = mean water depth. Lithology: WK = wackestone, PK = packstone, GR = grainstone, FL = floatstone, RD = rudstone. VPDB = Vienna Peedee belemnite international standard.
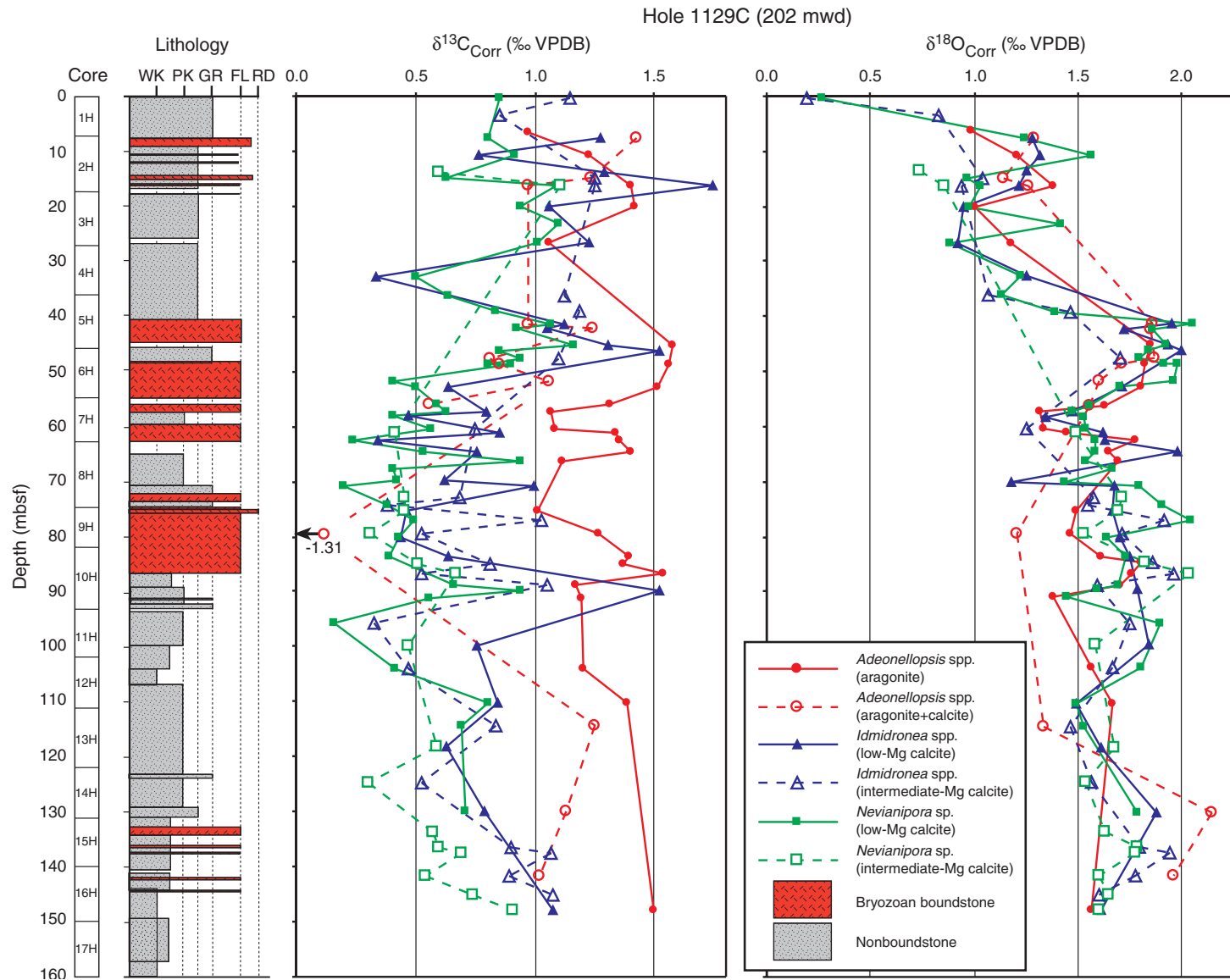
Figure F3. $\delta^{13}C_{corr}$ and $\delta^{18}O_{corr}$ profiles of three genera of bryozoans and simplified lithologic column of Hole 1131A. mwd = mean water depth. Lithology: WK = wackestone, PK = packstone, GR = grainstone, FL = floatstone, RD = rudstone. VPDB = Vienna Peedee belemnite international standard.
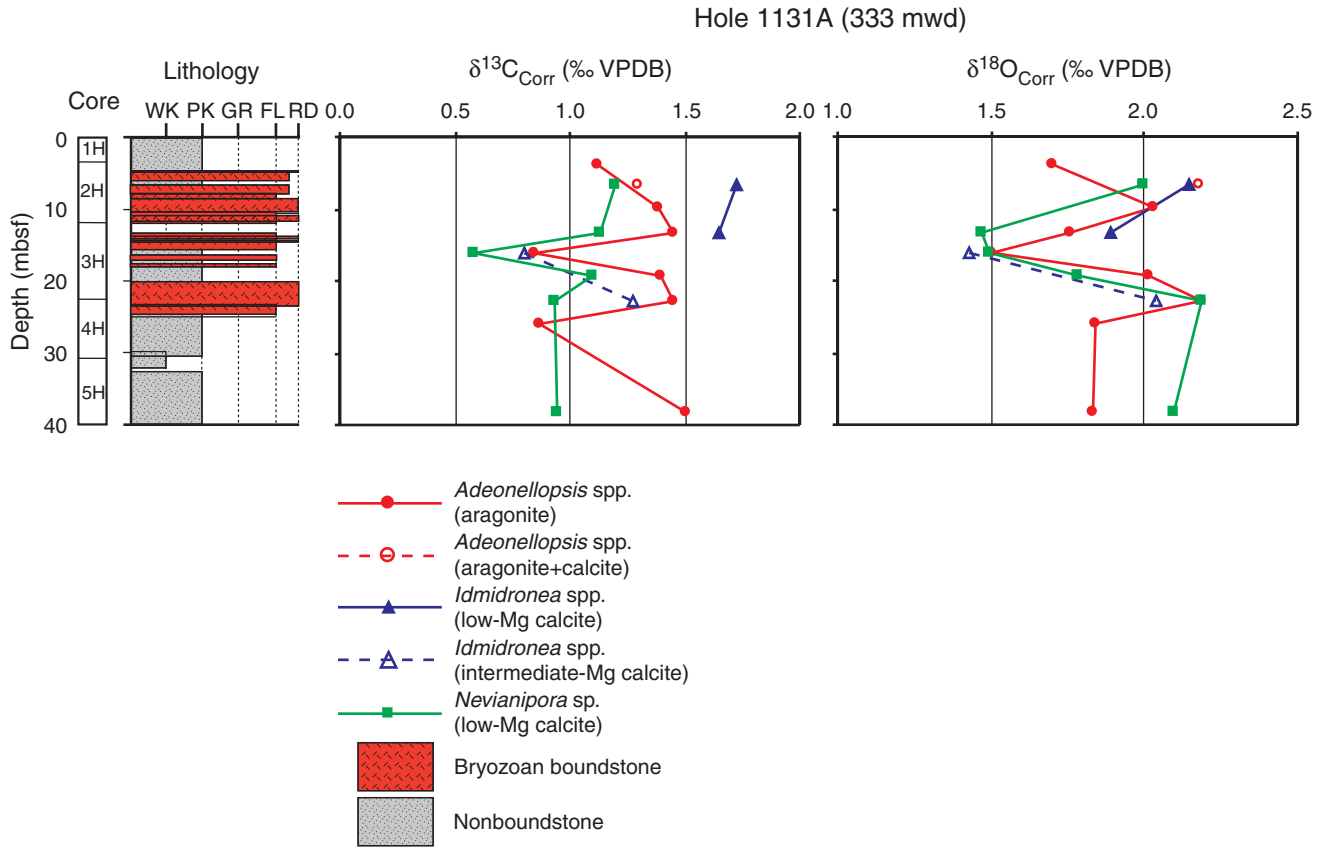
Figure F4. $\delta^{13}C_{corr}$ and $\delta^{18}O_{corr}$ profiles of three genera of bryozoans and simplified lithologic column of Hole 1132B. mwd = mean water depth. Lithology: WK = wackestone, PK = packstone, GR = grainstone, FL = floatstone, RD = rudstone. VPDB = Vienna Peedee belemnite international standard.
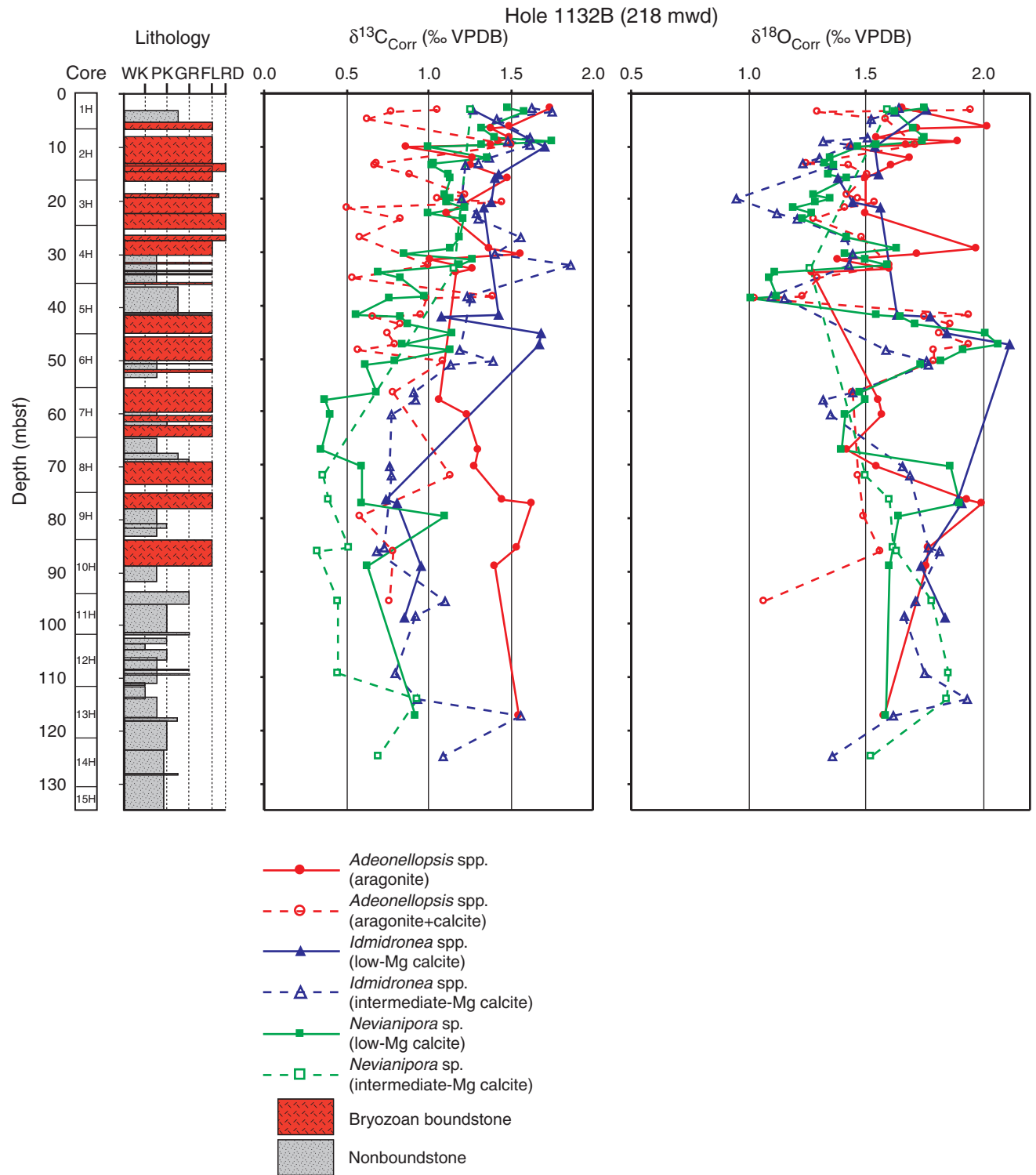
Figure F5. Scanning electron photomicrographs of the bryozoans examined in this study. **A.** Cyclostome *Nevianipora* sp. from 10.7 mbsf at Hole 1132B. **B.** Cyclostome *Idmidronea* spp. from 32.7 mbsf at Hole 1129C. **C.** Cheilostome *Adeonellopsis* spp. from 51.7 mbsf at Hole 1132B.

A

500 µm

B

200 µm

C
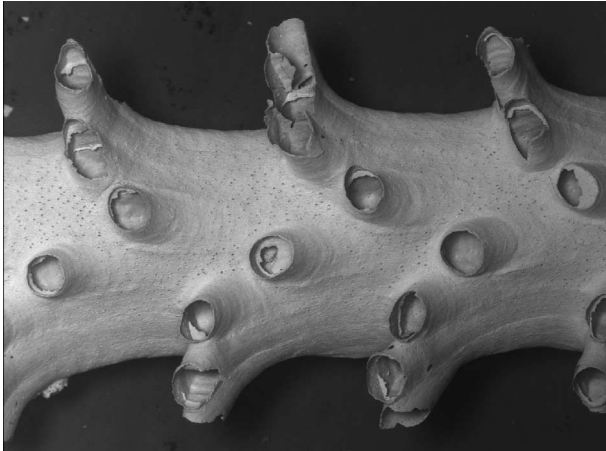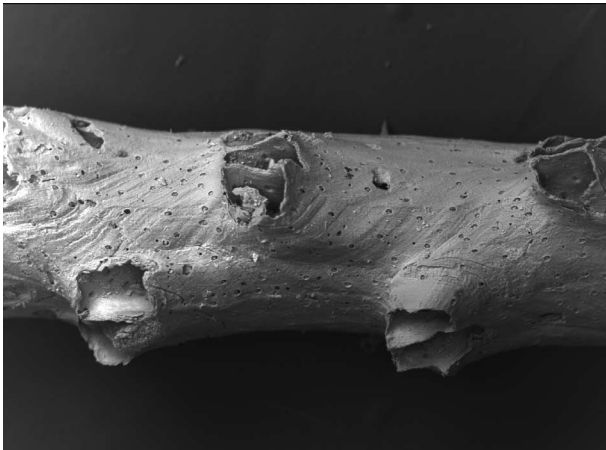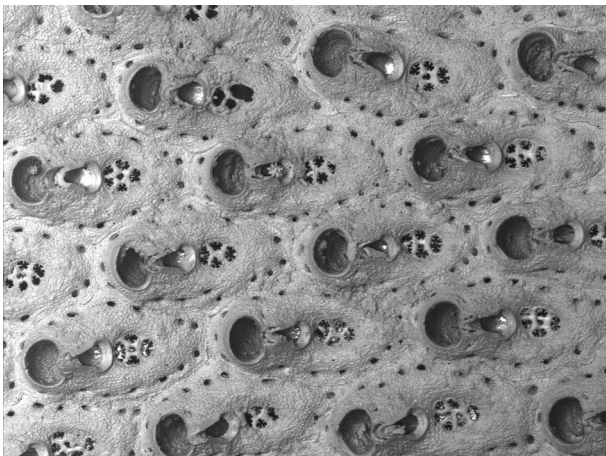
200 µm

Figure F6. Scanning electron photomicrographs of skeletons of *Nevianipora* sp. from Hole 1129C. **A.** 10.7 mbsf. **B.** 32.7 mbsf. **C.** 51.7 mbsf. **D.** 86.7 mbsf. Note, more marine cements (arrows) are found within intraskeletal spaces with increasing depth.
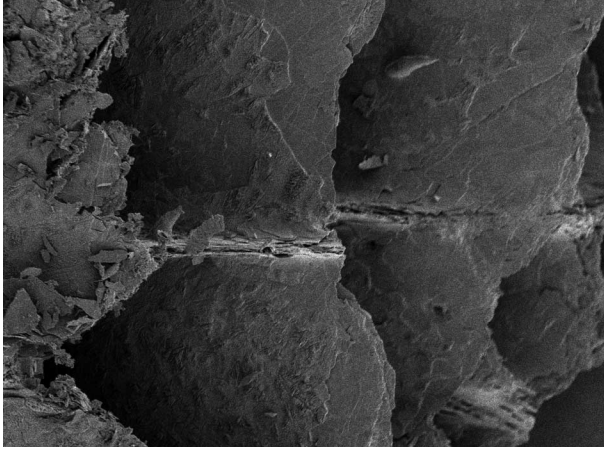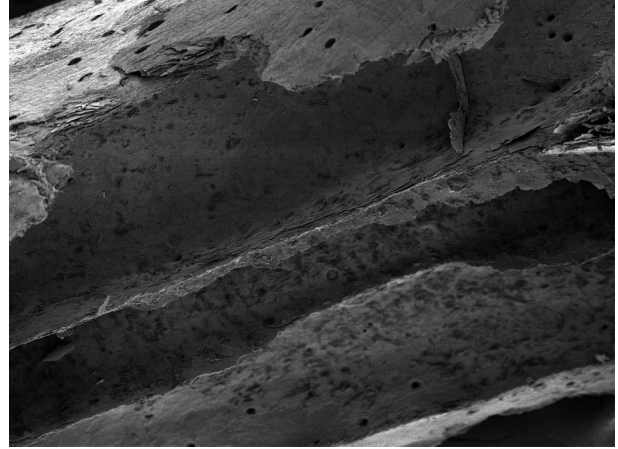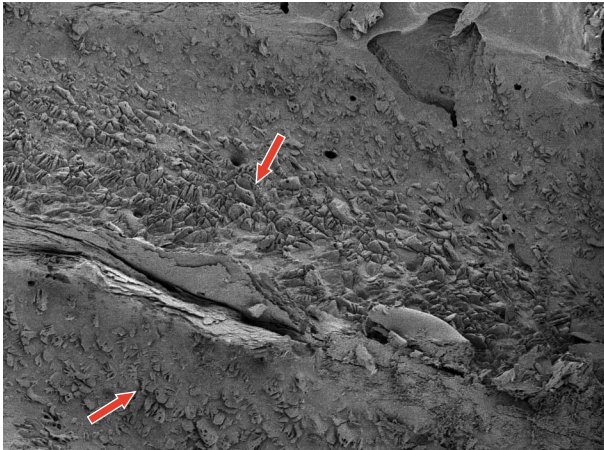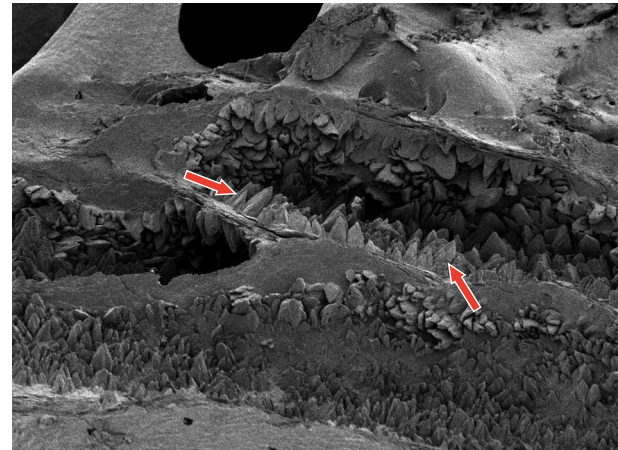
Figure F7. Comparisons of $\delta^{18}O$ ranges of equilibrium pure calcite and aragonite (shaded bars) and those of *Adeonellopsis* and *Nevianipora* (open circles). $\delta^{18}O$ values of *Nevianipora* are corrected for the effects of $MgCO_3$-dependent oxygen isotope fractionation (Tarutani et al., 1969). A number in the parentheses represents the "laboratory sample number" from Table 1 of Bone and James (1997).
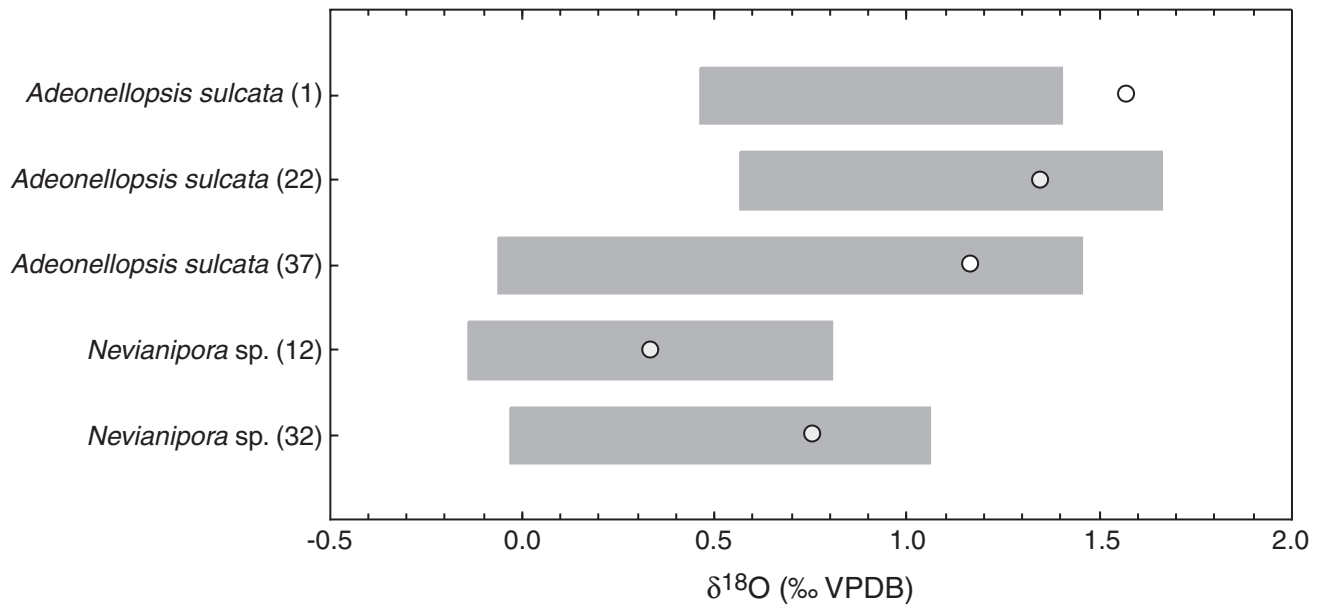
Figure F8. Relationships between carbonate mineralogy and isotopic composition of *Adeonellopsis*. **A.** Oxygen isotope. **B.** Carbon isotope. VPDB = Vienna Peedee belemnite international standard.
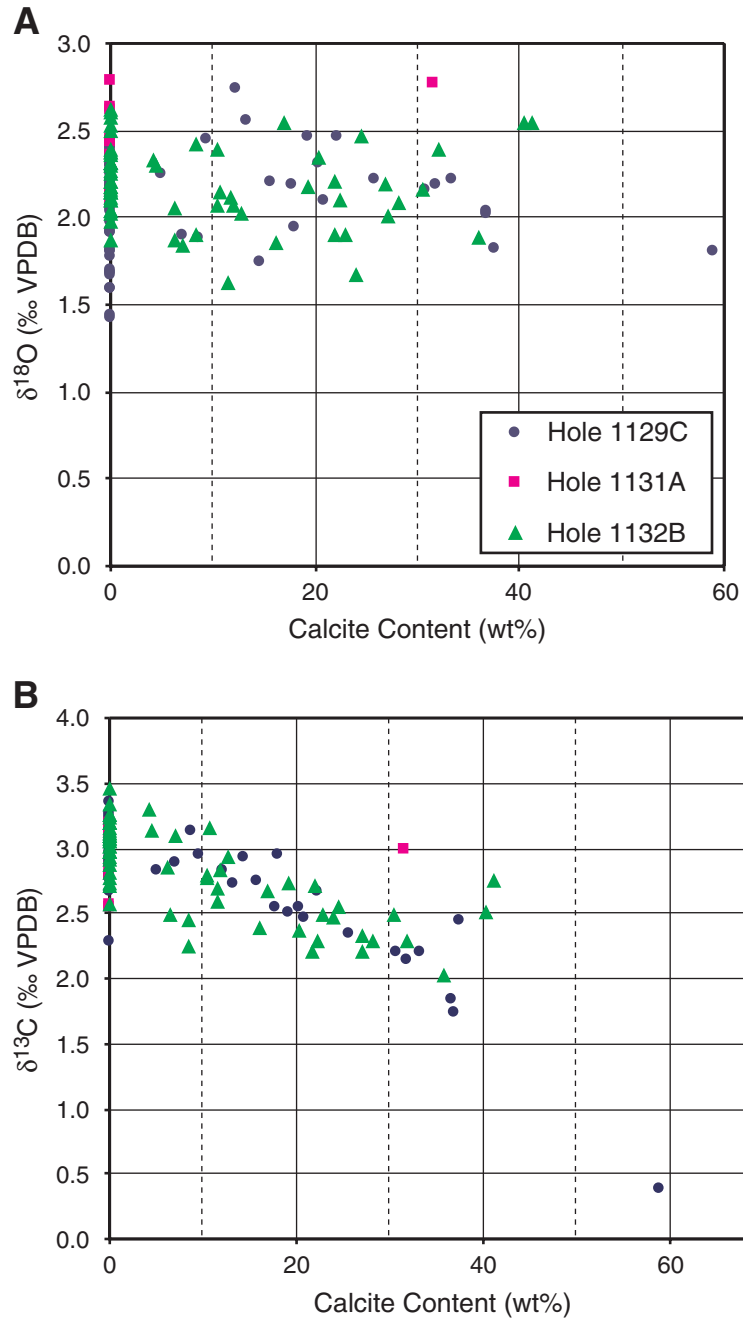
Figure F9. Correlation of bryozoan oxygen isotopic profiles from Holes 1129C, 1131A, and 1132B with the Quaternary oxygen isotopic record (Berger et al., 1994). Marine isotope stages are given in each profile. Shaded bars indicate the boundstone horizons. mwd = mean water depth. VPDB = Vienna Peedee belemnite international standard. ? = possible correlation with isotopic stage.
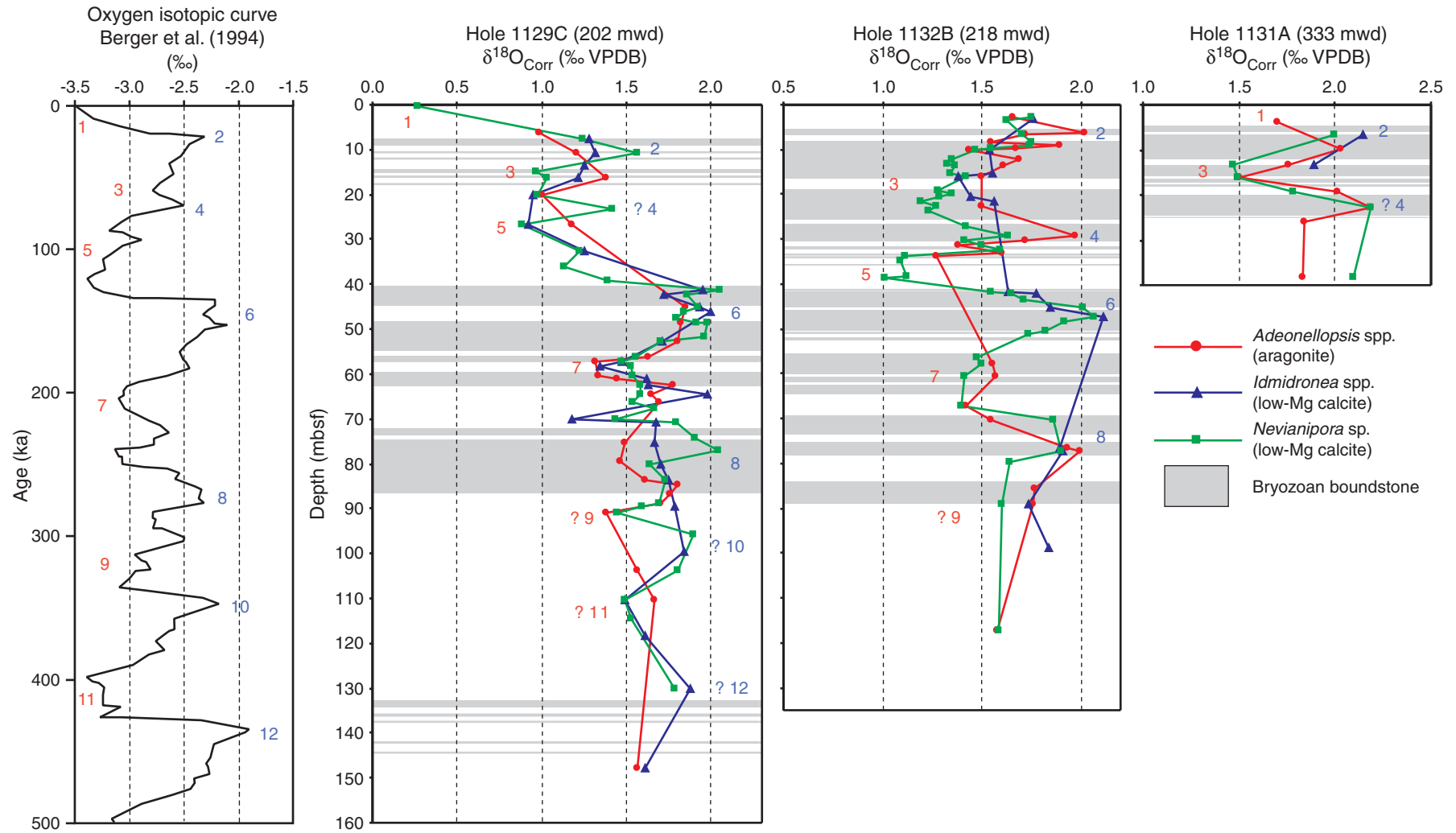
Table T1. Isotopic composition and carbonate mineralogy of bryozoans, Holes 1129C, 1131A and 1132B. (**See table notes.** Continued on next six pages.)

Core, section, interval (cm)	Depth (mbsf)	Bryozoan species	$\delta^{13}C$ (‰ VPDB)	$\delta^{18}O$ (‰ VPDB)	Mineralogy			$\delta^{13}C_{corr}$ (‰ VPDB)	$\delta^{18}O_{corr}$ (‰ VPDB)
					Aragonite (wt%)	Calcite (wt%)	Mg (mol%)		
182-1129C-									
1H-5, 40–42	6.40	*Adeonellopsis* spp.	2.67	1.59	100.0	0.0		0.97	0.99
2H-1, 40–42	7.70	*Adeonellopsis* spp.	3.13	1.89	91.4	8.6	11.8	1.43	1.29
2H-3, 40–42	10.70	*Adeonellopsis* spp.	2.93	1.81	100.0	0.0		1.23	1.21
2H-6, 08–12	14.88	*Adeonellopsis* spp.	2.93	1.74	85.5	14.5	10.9	1.23	1.14
2H-7, 02–6	16.32	*Adeonellopsis* spp.	2.45	1.82	62.3	37.7	9.7	0.75	1.22
2H-7, 02–6	16.32	*Adeonellopsis* spp.	2.89	1.89	92.8	7.2	10.4	1.19	1.29
2H-7, 02–6	16.32	*Adeonellopsis* spp.	3.01	1.80	100.0	0.0		1.31	1.20
2H-7, 02–6	16.32	*Adeonellopsis* spp.	3.21	1.92	100.0	0.0		1.51	1.32
2H-7, 02–6	16.32	*Adeonellopsis* spp.	3.05	2.15	100.0	0.0		1.35	1.55
2H-7, 02–6	16.32	*Adeonellopsis* spp.	3.09	2.22	100.0	0.0		1.39	1.62
2H-7, 02–6	16.32	*Adeonellopsis* spp.	3.15	1.82	100.0	0.0		1.45	1.22
3H-3, 40–42	20.20	*Adeonellopsis* spp.	3.21	1.69	100.0	0.0		1.51	1.09
3H-5, 40–42	23.20	*Adeonellopsis* spp.	3.08	1.66	100.0	0.0		1.38	1.06
3H-5, 40–42	23.20	*Adeonellopsis* spp.	3.07	1.44	100.0	0.0		1.37	0.84
3H-5, 40–42	23.20	*Adeonellopsis* spp.	3.07	1.69	100.0	0.0		1.37	1.09
3H-5, 40–42	23.20	*Adeonellopsis* spp.	3.18	1.42	100.0	0.0		1.48	0.82
3H-5, 40–42	23.20	*Adeonellopsis* spp.	3.06	1.68	100.0	0.0		1.36	1.08
3H-5, 40–42	23.20	*Adeonellopsis* spp.	3.14	1.60	100.0	0.0		1.44	1.00
4H-1, 40–42	26.70	*Adeonellopsis* spp.	2.76	1.78	100.0	0.0		1.06	1.18
5H-4, 112–116	41.42	*Adeonellopsis* spp.	2.68	2.46	77.7	22.3	7.6	0.98	1.86
5H-5, 40–42	42.20	*Adeonellopsis* spp.	2.94	2.45	90.5	9.5	10.3	1.24	1.85
5H-7, 32–36	45.12	*Adeonellopsis* spp.	3.27	2.45	100.0	0.0		1.57	1.85
6H-2, 83–87	47.63	*Adeonellopsis* spp.	2.51	2.47	80.8	19.2	9.1	0.81	1.87
6H-3, 40–42	48.70	*Adeonellopsis* spp.	3.26	2.42	100.0	0.0		1.56	1.82
6H-3, 40–42	48.72	*Adeonellopsis* spp.	2.55	2.31	79.6	20.4	10.1	0.85	1.71
6H-5, 40–42	51.70	*Adeonellopsis* spp.	2.76	2.20	84.3	15.7	11.3	1.06	1.60
6H-6, 02–6	52.82	*Adeonellopsis* spp.	3.22	2.40	100.0	0.0		1.52	1.80
7H-1, 133–137	56.13	*Adeonellopsis* spp.	2.20	2.15	69.2	30.8	9.2	0.50	1.55
7H-1, 133–137	56.13	*Adeonellopsis* spp.	2.35	2.22	74.2	25.8	8.4	0.65	1.62
7H-1, 133–137	56.13	*Adeonellopsis* spp.	2.20	2.22	66.7	33.3	9.6	0.50	1.62
7H-1, 133–137	56.13	*Adeonellopsis* spp.	1.74	2.02	63.1	36.9	9.8	0.04	1.42
7H-1, 133–137	56.13	*Adeonellopsis* spp.	1.84	2.04	63.2	36.8	8.8	0.14	1.44
7H-1, 133–137	56.13	*Adeonellopsis* spp.	2.46	2.10	79.1	20.9	10.2	0.76	1.50
7H-1, 133–137	56.13	*Adeonellopsis* spp.	2.55	2.19	82.2	17.8	9.8	0.85	1.59
7H-1, 133–137	56.13	*Adeonellopsis* spp.	2.83	2.24	95.1	4.9	11.4	1.13	1.64
7H-1, 133–137	56.13	*Adeonellopsis* spp.	2.88	2.15	100.0	0.0		1.18	1.55
7H-1, 133–137	56.13	*Adeonellopsis* spp.	2.14	2.19	68.1	31.9	10.3	0.44	1.59
7H-1, 133–137	56.13	*Adeonellopsis* spp.	2.88	2.37	100.0	0.0		1.18	1.77
7H-1, 133–137	56.13	*Adeonellopsis* spp.	3.01	2.17	100.0	0.0		1.31	1.57
7H-1, 133–137	56.13	*Adeonellopsis* spp.	3.09	2.21	100.0	0.0		1.39	1.61
7H-1, 133–137	56.13	*Adeonellopsis* spp.	3.10	2.29	100.0	0.0		1.40	1.69
7H-1, 133–137	56.13	*Adeonellopsis* spp.	3.14	2.17	100.0	0.0		1.44	1.57
7H-2, 114–118	57.44	*Adeonellopsis* spp.	2.77	1.92	100.0	0.0		1.07	1.32
7H-4, 124–128	60.54	*Adeonellopsis* spp.	2.79	1.93	100.0	0.0		1.09	1.33
7H-5, 40–42	61.20	*Adeonellopsis* spp.	3.04	2.04	100.0	0.0		1.34	1.44
7H-6, 41–43	62.41	*Adeonellopsis* spp.	3.06	2.37	100.0	0.0		1.36	1.77
8H-1, 40–42	64.70	*Adeonellopsis* spp.	3.11	2.13	100.0	0.0		1.41	1.53
8H-1, 40–42	64.70	*Adeonellopsis* spp.	3.10	2.24	100.0	0.0		1.40	1.64
8H-1, 40–42	64.70	*Adeonellopsis* spp.	3.36	2.36	100.0	0.0		1.66	1.76
8H-1, 40–42	64.70	*Adeonellopsis* spp.	3.11	2.16	100.0	0.0		1.41	1.56
8H-1, 40–42	64.70	*Adeonellopsis* spp.	3.00	2.13	100.0	0.0		1.30	1.53
8H-1, 40–42	64.70	*Adeonellopsis* spp.	3.03	2.41	100.0	0.0		1.33	1.81
8H-1, 40–42	64.70	*Adeonellopsis* spp.	3.01	2.19	100.0	0.0		1.31	1.59
8H-1, 40–42	64.70	*Adeonellopsis* spp.	3.08	2.38	100.0	0.0		1.38	1.78
8H-2, 45–49	66.25	*Adeonellopsis* spp.	2.82	2.29	100.0	0.0		1.12	1.69
9H-2, 06–10	75.36	*Adeonellopsis* spp.	2.28	2.03	100.0	0.0		0.58	1.43
9H-2, 06–10	75.36	*Adeonellopsis* spp.	3.16	2.15	100.0	0.0		1.46	1.55
9H-4, 122–126	79.52	*Adeonellopsis* spp.	0.39	1.80	41.0	59.0	9.1	–1.31	1.20
9H-4, 122–126	79.52	*Adeonellopsis* spp.	2.97	2.07	100.0	0.0		1.27	1.47
10H-1, 40–42	83.70	*Adeonellopsis* spp.	3.09	2.21	100.0	0.0		1.39	1.61
10H-2, 05–9	84.85	*Adeonellopsis* spp.	3.07	2.40	100.0	0.0		1.37	1.80
10H-3, 40–42	86.70	*Adeonellopsis* spp.	3.24	2.36	100.0	0.0		1.54	1.76
10H-4, 115–119	88.95	*Adeonellopsis* spp.	2.87	2.30	100.0	0.0		1.17	1.70
10H-6, 29–33	91.09	*Adeonellopsis* spp.	2.89	1.98	100.0	0.0		1.19	1.38
12H-2, 10–14	103.90	*Adeonellopsis* spp.	2.90	2.17	100.0	0.0		1.20	1.57
12H-6, 44–48	110.24	*Adeonellopsis* spp.	3.09	2.26	100.0	0.0		1.39	1.66

Table T1 (continued).

Core, section, interval (cm)	Depth (mbsf)	Bryozoan species	$\delta^{13}C$ (‰ VPDB)	$\delta^{18}O$ (‰ VPDB)	Mineralogy			$\delta^{13}C_{corr}$ (‰ VPDB)	$\delta^{18}O_{corr}$ (‰ VPDB)
					Aragonite (wt%)	Calcite (wt%)	Mg (mol%)		
13H-2, 113–117	114.43	*Adeonellopsis* spp.	2.95	1.94	82.0	18.0	6.8	1.25	1.34
14H-6, 123–127	130.03	*Adeonellopsis* spp.	2.83	2.75	87.9	12.1	10.2	1.13	2.15
16H-1, 126–130	141.56	*Adeonellopsis* spp.	2.72	2.56	86.7	13.3	8.9	1.02	1.96
16H-6, 02–6	147.82	*Adeonellopsis* spp.	3.20	2.17	100.0	0.0		1.50	1.57
182-1129C-									
1H-1, 40–42	0.40	*Idmidronea* spp.	1.15	0.53	0.0	100.0	5.7	1.15	0.19
1H-3, 40–42	3.40	*Idmidronea* spp.	0.85	1.09	0.0	100.0	4.3	0.85	0.83
2H-1, 40–42	7.70	*Idmidronea* spp.	1.28	1.52	0.0	100.0	4.0	1.28	1.28
2H-3, 40–42	10.70	*Idmidronea* spp.	0.76	1.41	0.0	100.0	1.6	0.76	1.31
2H-5, 40–42	13.70	*Idmidronea* spp.	1.29	1.37	0.0	100.0	2.1	1.29	1.25
2H-6, 08–12	14.88	*Idmidronea* spp.	1.25	1.30	0.0	100.0	4.3	1.25	1.04
2H-7, 02–6	16.32	*Idmidronea* spp.	1.74	1.39	0.0	100.0	2.8	1.74	1.22
2H-7, 02–6	16.32	*Idmidronea* spp.	0.98	1.38	0.0	100.0	10.0	0.98	0.78
2H-7, 02–6	16.32	*Idmidronea* spp.	1.26	1.38	0.0	100.0	4.4	1.26	1.11
2H-7, 02–6	16.32	*Idmidronea* spp.	1.40	1.13	0.0	100.0	6.0	1.40	0.77
2H-7, 02–6	16.32	*Idmidronea* spp.	1.40	1.24	0.0	100.0	6.0	1.40	0.88
2H-7, 02–6	16.32	*Idmidronea* spp.	1.18	1.36	0.0	100.0	6.4	1.18	0.98
2H-7, 02–6	16.32	*Idmidronea* spp.	1.34	1.40	0.0	100.0	4.7	1.34	1.11
2H-7, 02–6	16.32	*Idmidronea* spp.	1.16	1.16	0.0	100.0	6.7	1.16	0.76
2H-7, 02–6	16.32	*Idmidronea* spp.	1.13	1.09	0.0	100.0	4.9	1.13	0.79
2H-7, 02–6	16.32	*Idmidronea* spp.	1.22	1.27	0.0	100.0	4.8	1.22	0.98
2H-7, 02–6	16.32	*Idmidronea* spp.	1.31	1.51	0.0	100.0	5.1	1.31	1.20
2H-7, 02–6	16.32	*Idmidronea* spp.	1.42	1.39	0.0	100.0	7.1	1.42	0.96
3H-3, 40–42	20.20	*Idmidronea* spp.	1.06	1.16	0.0	100.0	3.5	1.06	0.95
4H-1, 40–42	26.70	*Idmidronea* spp.	1.23	1.16	0.0	100.0	3.9	1.23	0.92
4H-5, 40–42	32.70	*Idmidronea* spp.	0.34	1.34	0.0	100.0	1.5	0.34	1.25
5H-1, 40–42	36.20	*Idmidronea* spp.	1.12	1.32	0.0	100.0	4.2	1.12	1.07
5H-3, 40–42	39.20	*Idmidronea* spp.	1.19	1.74	0.0	100.0	4.5	1.19	1.47
5H-4, 112–116	41.42	*Idmidronea* spp.	1.12	2.09	0.0	100.0	2.4	1.12	1.95
5H-5, 40–42	42.20	*Idmidronea* spp.	1.05	1.97	0.0	100.0	4.0	1.05	1.72
5H-7, 32–36	45.12	*Idmidronea* spp.	1.31	2.14	0.0	100.0	3.6	1.31	1.93
6H-1, 40–42	46.19	*Idmidronea* spp.	1.52	2.15	0.0	100.0	2.6	1.52	1.99
6H-2, 83–87	47.63	*Idmidronea* spp.	1.10	2.07	0.0	100.0	6.2	1.10	1.70
6H-6, 02–6	52.82	*Idmidronea* spp.	0.64	1.91	0.0	100.0	3.3	0.64	1.71
7H-2, 114–118	57.44	*Idmidronea* spp.	0.80	1.68	0.0	100.0	3.5	0.80	1.47
7H-3, 40–42	58.20	*Idmidronea* spp.	0.47	1.49	0.0	100.0	2.4	0.47	1.34
7H-4, 124–128	60.54	*Idmidronea* spp.	0.75	1.71	0.0	100.0	7.6	0.75	1.25
7H-5, 40–42	61.20	*Idmidronea* spp.	0.85	1.83	0.0	100.0	3.5	0.85	1.62
7H-6, 41–43	62.41	*Idmidronea* spp.	0.35	1.80	0.0	100.0	2.9	0.35	1.62
8H-1, 40–42	64.70	*Idmidronea* spp.	0.75	2.13	0.0	100.0	2.4	0.75	1.98
8H-4, 114–118	69.94	*Idmidronea* spp.	0.62	1.42	0.0	100.0	3.9	0.62	1.18
8H-5, 40–42	70.70	*Idmidronea* spp.	1.00	1.87	0.0	100.0	3.3	1.00	1.67
8H-6, 101–105	72.81	*Idmidronea* spp.	0.68	1.91	0.0	100.0	5.5	0.68	1.58
9H-1, 40–42	74.20	*Idmidronea* spp.	0.38	1.89	0.0	100.0	5.6	0.38	1.55
9H-2, 06–10	75.36	*Idmidronea* spp.	0.47	1.89	0.0	100.0	3.8	0.47	1.66
9H-3, 40–42	77.20	*Idmidronea* spp.	1.03	2.30	0.0	100.0	6.3	1.03	1.92
9H-4, 122–126	79.52	*Idmidronea* spp.	0.53	2.01	0.0	100.0	5.0	0.53	1.71
9H-5, 40–42	80.20	*Idmidronea* spp.	0.44	1.91	0.0	100.0	3.5	0.44	1.70
10H-1, 40–42	83.70	*Idmidronea* spp.	0.64	1.93	0.0	100.0	3.1	0.64	1.75
10H-2, 05–9	84.85	*Idmidronea* spp.	0.81	2.12	0.0	100.0	4.4	0.81	1.86
10H-3, 40–42	86.70	*Idmidronea* spp.	0.52	2.30	0.0	100.0	5.5	0.52	1.96
10H-4, 115–119	88.95	*Idmidronea* spp.	1.05	1.90	0.0	100.0	5.2	1.05	1.59
10H-5, 40–42	89.70	*Idmidronea* spp.	1.52	2.00	0.0	100.0	3.5	1.52	1.79
11H-2, 140–144	95.70	*Idmidronea* spp.	0.32	2.07	0.0	100.0	5.3	0.32	1.75
11H-5, 92–96	99.72	*Idmidronea* spp.	0.76	2.03	0.0	100.0	3.1	0.76	1.84
12H-2, 10–14	103.90	*Idmidronea* spp.	0.47	2.03	0.0	100.0	6.1	0.47	1.66
12H-6, 44–48	110.24	*Idmidronea* spp.	0.85	1.73	0.0	100.0	4.0	0.85	1.49
13H-2, 113–117	114.43	*Idmidronea* spp.	0.84	1.72	0.0	100.0	4.2	0.84	1.47
13H-5, 40–42	118.20	*Idmidronea* spp.	0.63	1.85	0.0	100.0	4.0	0.63	1.61
14H-3, 40–42	124.70	*Idmidronea* spp.	0.52	1.87	0.0	100.0	5.2	0.52	1.56
14H-6, 123–127	130.03	*Idmidronea* spp.	0.79	2.11	0.0	100.0	3.8	0.79	1.88
15H-4, 111–115	136.41	*Idmidronea* spp.	0.90	2.07	0.0	100.0	4.5	0.90	1.79
15H-5, 79–81	137.59	*Idmidronea* spp.	1.07	2.19	0.0	100.0	4.1	1.07	1.94
16H-1, 126–130	141.56	*Idmidronea* spp.	0.89	2.10	0.0	100.0	5.5	0.89	1.77
16H-4, 40–42	145.20	*Idmidronea* spp.	1.08	1.92	0.0	100.0	5.2	1.08	1.60
16H-6, 02–6	147.82	*Idmidronea* spp.	1.08	1.85	0.0	100.0	4.0	1.08	1.61

Table T1 (continued).

Core, section, interval (cm)	Depth (mbsf)	Bryozoan species	δ13C (‰ VPDB)	δ18O (‰ VPDB)	Mineralogy Aragonite (wt%)	Calcite (wt%)	Mg (mol%)	δ13Ccorr (‰ VPDB)	δ18Ocorr (‰ VPDB)
182-1129C-									
1H-1, 40–42	0.40	*Nevianipora* sp.	0.85	0.43	0.0	100.0	2.7	0.85	0.27
2H-1, 40–42	7.70	*Nevianipora* sp.	0.81	1.34	0.0	100.0	1.6	0.81	1.24
2H-3, 40–42	10.70	*Nevianipora* sp.	0.92	1.61	0.0	100.0	0.9	0.92	1.56
2H-5, 40–42	13.70	*Nevianipora* sp.	0.59	1.10	0.0	100.0	6.2	0.59	0.73
2H-6, 08–12	14.88	*Nevianipora* sp.	0.63	1.12	0.0	100.0	2.5	0.63	0.96
2H-7, 02–6	16.32	*Nevianipora* sp.	1.15	1.14	0.0	100.0	2.9	1.15	0.96
2H-7, 02–6	16.32	*Nevianipora* sp.	1.13	1.18	0.0	100.0	4.3	1.13	0.92
2H-7, 02–6	16.32	*Nevianipora* sp.	1.61	1.26	0.0	100.0	3.4	1.61	1.06
2H-7, 02–6	16.32	*Nevianipora* sp.	1.22	1.37	0.0	100.0	5.7	1.22	1.03
2H-7, 02–6	16.32	*Nevianipora* sp.	1.02	1.26	0.0	100.0	2.2	1.02	1.13
2H-7, 02–6	16.32	*Nevianipora* sp.	0.64	1.21	0.0	100.0	2.4	0.64	1.06
2H-7, 02–6	16.32	*Nevianipora* sp.	0.92	0.97	0.0	100.0	6.4	0.92	0.58
2H-7, 02–6	16.32	*Nevianipora* sp.	1.07	1.17	0.0	100.0	5.1	1.07	0.86
2H-7, 02–6	16.32	*Nevianipora* sp.	0.96	1.18	0.0	100.0	2.8	0.96	1.01
2H-7, 02–6	16.32	*Nevianipora* sp.	1.20	1.15	0.0	100.0	4.4	1.20	0.88
2H-7, 02–6	16.32	*Nevianipora* sp.	1.17	1.12	0.0	100.0	2.6	1.17	0.97
3H-3, 40–42	20.20	*Nevianipora* sp.	0.94	1.09	0.0	100.0	1.9	0.94	0.98
3H-5, 40–42	23.20	*Nevianipora* sp.	1.10	1.53	0.0	100.0	2.0	1.10	1.41
4H-1, 40–42	26.70	*Nevianipora* sp.	1.01	1.04	0.0	100.0	2.6	1.01	0.89
4H-5, 40–42	32.70	*Nevianipora* sp.	0.50	1.29	0.0	100.0	1.1	0.50	1.22
5H-1, 40–42	36.20	*Nevianipora* sp.	0.63	1.29	0.0	100.0	2.5	0.63	1.14
5H-3, 40–42	39.20	*Nevianipora* sp.	0.83	1.51	0.0	100.0	2.1	0.83	1.39
5H-4, 112–116	41.42	*Nevianipora* sp.	1.06	2.16	0.0	100.0	1.8	1.06	2.05
5H-5, 40–42	42.20	*Nevianipora* sp.	0.92	2.01	0.0	100.0	2.5	0.92	1.85
5H-7, 32–36	45.12	*Nevianipora* sp.	1.16	2.13	0.0	100.0	3.4	1.16	1.92
6H-1, 40–42	46.19	*Nevianipora* sp.	0.86	1.90	0.0	100.0	0.9	0.86	1.84
6H-2, 83–87	47.63	*Nevianipora* sp.	0.94	2.02	0.0	100.0	3.7	0.94	1.79
6H-3, 40–42	48.70	*Nevianipora* sp.	0.80	2.03	0.0	100.0	2.0	0.80	1.91
6H-3, 42–44	48.72	*Nevianipora* sp.	0.90	2.04	0.0	100.0	1.0	0.90	1.98
6H-5, 40–42	51.70	*Nevianipora* sp.	0.40	2.09	0.0	100.0	2.1	0.40	1.96
6H-6, 02–6	52.82	*Nevianipora* sp.	0.50	1.80	0.0	100.0	1.6	0.50	1.70
7H-1, 133–137	56.13	*Nevianipora* sp.	0.59	1.71	0.0	100.0	2.7	0.59	1.55
7H-2, 114–118	57.44	*Nevianipora* sp.	0.63	1.59	0.0	100.0	2.1	0.63	1.47
7H-3, 40–42	58.20	*Nevianipora* sp.	0.41	1.58	0.0	100.0	0.9	0.41	1.53
7H-4, 124–128	60.54	*Nevianipora* sp.	0.57	1.72	0.0	100.0	3.1	0.57	1.53
7H-5, 40–42	61.20	*Nevianipora* sp.	0.42	1.75	0.0	100.0	4.3	0.42	1.49
7H-6, 41–43	62.41	*Nevianipora* sp.	0.24	1.78	0.0	100.0	3.3	0.24	1.58
8H-1, 40–42	64.70	*Nevianipora* sp.	0.53	1.79	0.0	100.0	3.5	0.53	1.58
8H-2, 45–49	66.25	*Nevianipora* sp.	0.94	1.70	0.0	100.0	2.6	0.94	1.54
8H-3, 40–42	67.70	*Nevianipora* sp.	0.41	1.74	0.0	100.0	1.2	0.41	1.67
8H-4, 114–118	69.94	*Nevianipora* sp.	0.42	1.62	0.0	100.0	3.1	0.42	1.44
8H-5, 40–42	70.70	*Nevianipora* sp.	0.20	2.01	0.0	100.0	3.6	0.20	1.80
8H-6, 101–105	72.81	*Nevianipora* sp.	0.45	1.95	0.0	100.0	4.1	0.45	1.71
9H-1, 40–42	74.20	*Nevianipora* sp.	0.39	2.14	0.0	100.0	3.9	0.39	1.91
9H-2, 06–10	75.36	*Nevianipora* sp.	0.45	1.97	0.0	100.0	4.6	0.45	1.69
9H-3, 40–42	77.20	*Nevianipora* sp.	0.49	2.23	0.0	100.0	3.1	0.49	2.04
9H-4, 122–126	79.52	*Nevianipora* sp.	0.31	1.83	0.0	100.0	4.9	0.31	1.53
9H-5, 40–42	80.20	*Nevianipora* sp.	0.43	1.87	0.0	100.0	3.8	0.43	1.64
10H-1, 40–42	83.70	*Nevianipora* sp.	0.39	1.96	0.0	100.0	3.8	0.39	1.73
10H-2, 05–9	84.85	*Nevianipora* sp.	0.51	2.08	0.0	100.0	4.3	0.51	1.82
10H-3, 40–42	86.70	*Nevianipora* sp.	0.67	2.33	0.0	100.0	5.0	0.67	2.03
10H-4, 115–119	88.95	*Nevianipora* sp.	0.67	1.78	0.0	100.0	1.4	0.67	1.69
10H-5, 40–42	89.70	*Nevianipora* sp.	0.94	1.73	0.0	100.0	2.2	0.94	1.59
10H-6, 29–33	91.09	*Nevianipora* sp.	0.56	1.58	0.0	100.0	2.3	0.56	1.45
11H-2, 140–144	95.70	*Nevianipora* sp.	0.16	2.03	0.0	100.0	2.1	0.16	1.90
11H-5, 92–96	99.72	*Nevianipora* sp.	0.47	1.89	0.0	100.0	5.1	0.47	1.59
12H-2, 10–14	103.90	*Nevianipora* sp.	0.41	2.03	0.0	100.0	3.8	0.41	1.80
12H-6, 44–48	110.24	*Nevianipora* sp.	0.81	1.67	0.0	100.0	2.9	0.81	1.49
13H-2, 113–117	114.43	*Nevianipora* sp.	0.69	1.72	0.0	100.0	3.1	0.69	1.53
13H-5, 40–42	118.20	*Nevianipora* sp.	0.59	1.97	0.0	100.0	4.8	0.59	1.68
14H-3, 40–42	124.70	*Nevianipora* sp.	0.31	1.86	0.0	100.0	5.3	0.31	1.54
14H-6, 123–127	130.03	*Nevianipora* sp.	0.71	2.01	0.0	100.0	3.6	0.71	1.79
15H-2, 130–134	133.60	*Nevianipora* sp.	0.57	2.01	0.0	100.0	6.3	0.57	1.63
15H-4, 111–115	136.41	*Nevianipora* sp.	0.60	2.03	0.0	100.0	4.1	0.60	1.79
15H-5, 79–81	137.59	*Nevianipora* sp.	0.69	2.05	0.0	100.0	4.5	0.69	1.78
16H-1, 126–130	141.56	*Nevianipora* sp.	0.54	1.96	0.0	100.0	6.0	0.54	1.60
16H-4, 40–42	145.20	*Nevianipora* sp.	0.74	1.92	0.0	100.0	4.5	0.74	1.64
16H-6, 02–6	147.82	*Nevianipora* sp.	0.91	1.86	0.0	100.0	4.4	0.91	1.60

Table T1 (continued).

Core, section, interval (cm)	Depth (mbsf)	Bryozoan species	δ¹³C (‰ VPDB)	δ¹⁸O (‰ VPDB)	Mineralogy Aragonite (wt%)	Calcite (wt%)	Mg (mol%)	δ¹³C$_{corr}$ (‰ VPDB)	δ¹⁸O$_{corr}$ (‰ VPDB)
182-1131A-									
2H-1, 40–42	3.80	*Adeonellopsis* spp.	2.85	2.45	100.0	0.0		1.15	1.85
2H-1, 40–42	3.80	*Adeonellopsis* spp.	2.79	2.14	100.0	0.0		1.09	1.54
2H-3, 40–42	6.80	*Adeonellopsis* spp.	2.99	2.78	68.4	31.6	9.1	1.29	2.18
2H-5, 40–42	9.85	*Adeonellopsis* spp.	3.08	2.63	100.0	0.0		1.38	2.03
3H-1, 40–42	13.30	*Adeonellopsis* spp.	3.16	2.36	100.0	0.0		1.46	1.76
3H-3, 40–42	16.30	*Adeonellopsis* spp.	2.55	2.10	100.0	0.0		0.85	1.50
3H-5, 40–42	19.30	*Adeonellopsis* spp.	3.10	2.62	100.0	0.0		1.40	2.02
4H-1, 40–42	22.80	*Adeonellopsis* spp.	3.16	2.79	100.0	0.0		1.46	2.19
4H-3, 40–42	25.80	*Adeonellopsis* spp.	2.56	2.44	100.0	0.0		0.86	1.84
5H-5, 40–42	38.30	*Adeonellopsis* spp.	3.20	2.44	100.0	0.0		1.50	1.84
182-1131A-									
2H-3, 40–42	6.80	*Idmidronea* spp.	1.73	2.37	0.0	100.0	3.9	1.73	2.14
3H-1, 40–42	13.30	*Idmidronea* spp.	1.65	2.08	0.0	100.0	3.3	1.65	1.89
3H-3, 40–42	16.30	*Idmidronea* spp.	0.81	1.73	0.0	100.0	5.0	0.81	1.43
4H-1, 40–42	22.80	*Idmidronea* spp.	1.28	2.30	0.0	100.0	4.3	1.28	2.04
5H-3, 40–42	35.30	*Idmidronea* spp.	0.39	2.09	0.0	100.0	NA	0.39	(2.09)
182-1131A-									
2H-3, 40–42	6.80	*Nevianipora* sp.	1.20	2.13	0.0	100.0	2.1	1.20	2.00
3H-1, 40–42	13.30	*Nevianipora* sp.	1.14	1.66	0.0	100.0	3.3	1.14	1.47
3H-3, 40–42	16.30	*Nevianipora* sp.	0.58	1.65	0.0	100.0	2.5	0.58	1.50
3H-5, 40–42	19.30	*Nevianipora* sp.	1.10	1.93	0.0	100.0	2.5	1.10	1.79
4H-1, 40–42	22.80	*Nevianipora* sp.	0.94	2.31	0.0	100.0	2.1	0.94	2.19
5H-3, 40–42	35.30	*Nevianipora* sp.	0.54	1.94	0.0	100.0	NA	0.54	(1.94)
5H-5, 40–42	38.30	*Nevianipora* sp.	0.95	2.24	0.0	100.0	2.3	0.95	2.10
182-1132B-									
1H-2, 123–127	2.73	*Adeonellopsis* spp.	3.45	2.26	100.0	0.0		1.75	1.66
1H-3, 07–11	3.07	*Adeonellopsis* spp.	2.75	2.54	58.8	41.2	11.6	1.05	1.94
1H-3, 40–42	3.40	*Adeonellopsis* spp.	2.48	1.90	77.1	22.9	11.1	0.78	1.30
1H-4, 54–58	5.04	*Adeonellopsis* spp.	2.32	2.18	73.0	27.0	9.1	0.62	1.58
1H-5, 40–42	6.40	*Adeonellopsis* spp.	3.19	2.62	100.0	0.0		1.49	2.02
1H-5, 50–54	6.50	*Adeonellopsis* spp.	3.08	2.32	100.0	0.0		1.38	1.72
2H-1, 146–150	8.26	*Adeonellopsis* spp.	3.19	2.15	100.0	0.0		1.49	1.55
2H-2, 76–80	9.06	*Adeonellopsis* spp.	3.12	2.50	100.0	0.0		1.42	1.90
2H-3, 04–8	9.84	*Adeonellopsis* spp.	3.13	2.30	95.5	4.5	10.3	1.43	1.70
2H-3, 04–8	9.84	*Adeonellopsis* spp.	3.28	2.32	95.9	4.1	12.1	1.58	1.72
2H-3, 04–8	9.84	*Adeonellopsis* spp.	3.12	2.31	100.0	0.0		1.42	1.71
2H-3, 04–8	9.84	*Adeonellopsis* spp.	3.10	2.24	100.0	0.0		1.40	1.64
2H-3, 04–8	9.84	*Adeonellopsis* spp.	3.08	2.14	100.0	0.0		1.38	1.54
2H-3, 04–8	9.84	*Adeonellopsis* spp.	3.04	2.38	100.0	0.0		1.34	1.78
2H-3, 40–42	10.20	*Adeonellopsis* spp.	2.57	2.04	100.0	0.0		0.87	1.44
2H-4, 72–76	12.02	*Adeonellopsis* spp.	2.97	2.29	100.0	0.0		1.27	1.69
2H-5, 40–42	13.20	*Adeonellopsis* spp.	2.39	1.85	83.8	16.2	9.9	0.69	1.25
2H-5, 81–85	13.61	*Adeonellopsis* spp.	2.02	1.88	64.1	35.9	7.8	0.32	1.28
2H-5, 81–85	13.61	*Adeonellopsis* spp.	3.02	2.12	100.0	0.0		1.32	1.52
2H-5, 81–85	13.61	*Adeonellopsis* spp.	3.05	2.38	100.0	0.0		1.35	1.78
2H-5, 81–85	13.61	*Adeonellopsis* spp.	2.74	2.18	80.7	19.3	10.9	1.04	1.58
2H-5, 81–85	13.61	*Adeonellopsis* spp.	2.74	2.20	100.0	0.0		1.04	1.60
2H-5, 81–85	13.61	*Adeonellopsis* spp.	2.91	2.03	100.0	0.0		1.21	1.43
2H-5, 81–85	13.61	*Adeonellopsis* spp.	3.10	2.31	100.0	0.0		1.40	1.71
2H-6, 96–100	15.26	*Adeonellopsis* spp.	2.59	2.11	88.3	11.7	11.7	0.89	1.51
2H-CC, 05–7	16.12	*Adeonellopsis* spp.	3.18	2.10	100.0	0.0		1.48	1.50
3H-2, 146–150	19.26	*Adeonellopsis* spp.	2.92	2.02	87.3	12.7	10.7	1.22	1.42
3H-3, 40–42	19.70	*Adeonellopsis* spp.	2.76	2.07	89.6	10.4	10.4	1.06	1.47
3H-3, 130–134	20.60	*Adeonellopsis* spp.	3.15	2.14	89.2	10.8	8.6	1.45	1.54
3H-4, 72–76	21.52	*Adeonellopsis* spp.	2.21	2.01	72.9	27.1	10.6	0.51	1.41
3H-5, 40–42	22.70	*Adeonellopsis* spp.	2.82	2.10	100.0	0.0		1.12	1.50
3H-5, 123–125	23.53	*Adeonellopsis* spp.	2.20	1.89	78.1	21.9	7.9	0.50	1.29
3H-5, 123–125	23.53	*Adeonellopsis* spp.	2.86	1.86	93.8	6.2	7.5	1.16	1.26
4H-1, 146–150	27.26	*Adeonellopsis* spp.	2.28	2.09	71.9	28.1	9.8	0.58	1.49
4H-3, 40–42	29.20	*Adeonellopsis* spp.	3.08	2.57	100.0	0.0		1.38	1.97
4H-4, 01–3	30.31	*Adeonellopsis* spp.	3.26	2.32	100.0	0.0		1.56	1.72
4H-4, 89–93	31.19	*Adeonellopsis* spp.	2.71	1.98	100.0	0.0		1.01	1.38
4H-5, 40–42	32.20	*Adeonellopsis* spp.	2.70	2.20	78.1	21.9	9.2	1.00	1.60
4H-5, 142–144	33.22	*Adeonellopsis* spp.	2.97	2.20	100.0	0.0		1.27	1.60
4H-6, 46–50	33.76	*Adeonellopsis* spp.	2.87	1.87	100.0	0.0		1.17	1.27
4H-7, 50–54	34.80	*Adeonellopsis* spp.	2.24	1.90	91.6	8.4	9.3	0.54	1.30

Table T1 (continued).

Core, section, interval (cm)	Depth (mbsf)	Bryozoan species	$\delta^{13}C$ (‰ VPDB)	$\delta^{18}O$ (‰ VPDB)	Mineralogy			$\delta^{13}C_{corr}$ (‰ VPDB)	$\delta^{18}O_{corr}$ (‰ VPDB)
					Aragonite (wt%)	Calcite (wt%)	Mg (mol%)		
5H-2, 146–150	38.26	*Adeonellopsis* spp.	3.09	1.83	92.9	7.1	9.2	1.39	1.23
5H-3, 40–42	38.70	*Adeonellopsis* spp.	2.69	1.63	88.5	11.5	7.5	0.99	1.03
5H-5, 40–42	41.70	*Adeonellopsis* spp.	2.66	2.54	83.0	17.0	10.5	0.96	1.94
5H-5, 66–70	41.96	*Adeonellopsis* spp.	2.36	2.35	79.6	20.4	8.5	0.66	1.75
5H-6, 75–79	43.55	*Adeonellopsis* spp.	2.54	2.46	75.5	24.5	9.5	0.84	1.86
6H-1, 41–43	45.21	*Adeonellopsis* spp.	2.45	2.42	91.6	8.4	9.9	0.75	1.82
6H-2, 87–91	47.17	*Adeonellopsis* spp.	2.50	2.54	59.6	40.4	6.9	0.80	1.94
6H-3, 40–42	48.20	*Adeonellopsis* spp.	2.28	2.39	68.0	32.0	6.9	0.58	1.79
6H-4, 130–134	50.60	*Adeonellopsis* spp.	2.79	2.39	89.6	10.4	10.7	1.09	1.79
7H-2, 67–71	56.47	*Adeonellopsis* spp.	2.48	2.04	93.6	6.4	8.1	0.78	1.44
7H-3, 40–42	57.70	*Adeonellopsis* spp.	2.77	2.15	100.0	0.0		1.07	1.55
7H-5, 40–42	60.70	*Adeonellopsis* spp.	2.94	2.17	100.0	0.0		1.24	1.57
8H-3, 40–42	67.20	*Adeonellopsis* spp.	3.01	2.02	100.0	0.0		1.31	1.42
8H-5, 40–42	70.20	*Adeonellopsis* spp.	2.98	2.15	100.0	0.0		1.28	1.55
8H-6, 68–72	71.98	*Adeonellopsis* spp.	2.83	2.07	88.0	12.0	10.0	1.13	1.47
9H-3, 40–42	76.70	*Adeonellopsis* spp.	3.15	2.53	100.0	0.0		1.45	1.93
9H-3, 105–109	77.35	*Adeonellopsis* spp.	3.33	2.60	100.0	0.0		1.63	2.00
9H-5, 40–42	79.70	*Adeonellopsis* spp.	2.28	2.09	77.6	22.4	6.7	0.58	1.49
10H-2, 139–143	85.69	*Adeonellopsis* spp.	3.24	2.37	100.0	0.0		1.54	1.77
10H-3, 40–42	86.20	*Adeonellopsis* spp.	2.48	2.16	69.5	30.5	8.2	0.78	1.56
10H-5, 40–42	89.20	*Adeonellopsis* spp.	3.11	2.36	100.0	0.0		1.41	1.76
11H-3, 40–42	95.70	*Adeonellopsis* spp.	2.47	1.67	75.9	24.1	9.9	0.77	1.07
13H-4, 130–134	117.10	*Adeonellopsis* spp.	3.26	2.18	100.0	0.0		1.56	1.58
182-1132B-									
1H-2, 123–127	2.73	*Idmidronea* spp.	1.63	1.95	0.0	100.0	5.1	1.63	1.64
1H-3, 07–11	3.07	*Idmidronea* spp.	1.27	1.97	0.0	100.0	3.5	1.27	1.76
1H-3, 40–42	3.40	*Idmidronea* spp.	1.75	1.90	0.0	100.0	4.6	1.75	1.62
1H-4, 54–58	5.04	*Idmidronea* spp.	1.41	1.80	0.0	100.0	4.6	1.41	1.52
2H-1, 146–150	8.26	*Idmidronea* spp.	1.62	1.84	0.0	100.0	5.5	1.62	1.51
2H-2, 76–80	9.06	*Idmidronea* spp.	1.49	1.58	0.0	100.0	4.3	1.49	1.32
2H-3, 04–8	9.84	*Idmidronea* spp.	1.60	1.86	0.0	100.0	10.1	1.60	1.26
2H-3, 04–8	9.84	*Idmidronea* spp.	1.76	1.69	0.0	100.0	9.6	1.76	1.12
2H-3, 04–8	9.84	*Idmidronea* spp.	1.86	1.87	0.0	100.0	8.0	1.86	1.38
2H-3, 04–8	9.84	*Idmidronea* spp.	1.24	1.72	0.0	100.0	5.2	1.24	1.41
2H-3, 04–8	9.84	*Idmidronea* spp.	1.39	1.92	0.0	100.0	5.7	1.39	1.58
2H-3, 04–8	9.84	*Idmidronea* spp.	1.80	1.96	0.0	100.0	5.3	1.80	1.64
2H-3, 04–8	9.84	*Idmidronea* spp.	1.53	1.89	0.0	100.0	8.2	1.53	1.40
2H-3, 04–8	9.84	*Idmidronea* spp.	1.42	1.79	0.0	100.0	8.6	1.42	1.27
2H-3, 04–8	9.84	*Idmidronea* spp.	1.77	2.29	0.0	100.0	4.5	1.77	2.02
2H-3, 04–8	9.84	*Idmidronea* spp.	1.69	1.86	0.0	100.0	4.8	1.69	1.58
2H-3, 04–8	9.84	*Idmidronea* spp.	1.76	1.47	0.0	100.0	5.5	1.76	1.14
2H-3, 40–42	10.20	*Idmidronea* spp.	1.71	1.77	0.0	100.0	3.8	1.71	1.54
2H-4, 72–76	12.02	*Idmidronea* spp.	1.37	1.64	0.0	100.0	5.6	1.37	1.31
2H-5, 40–42	13.20	*Idmidronea* spp.	1.31	1.55	0.0	100.0	5.2	1.31	1.23
2H-5, 81–85	13.61	*Idmidronea* spp.	1.23	1.67	0.0	100.0	5.2	1.23	1.36
2H-6, 96–100	15.26	*Idmidronea* spp.	1.42	1.78	0.0	100.0	3.8	1.42	1.55
2H-CC, 05–7	16.12	*Idmidronea* spp.	1.41	1.59	0.0	100.0	3.4	1.41	1.38
3H-3, 40–42	19.70	*Idmidronea* spp.	1.21	1.30	0.0	100.0	5.9	1.21	0.95
3H-3, 130–134	20.60	*Idmidronea* spp.	1.38	1.66	0.0	100.0	3.6	1.38	1.45
3H-4, 702–76	21.52	*Idmidronea* spp.	1.33	1.79	0.0	100.0	3.8	1.33	1.56
3H-5, 40–42	22.70	*Idmidronea* spp.	1.29	1.42	0.0	100.0	5.0	1.29	1.12
3H-5, 123–125	23.53	*Idmidronea* spp.	1.31	1.48	0.0	100.0	4.4	1.31	1.21
4H-1, 146–150	27.26	*Idmidronea* spp.	1.56	1.81	0.0	100.0	6.7	1.56	1.41
4H-4, 01–3	30.31	*Idmidronea* spp.	1.41	1.91	0.0	100.0	7.7	1.41	1.45
4H-5, 40–42	32.20	*Idmidronea* spp.	1.87	1.68	0.0	100.0	4.2	1.87	1.43
5H-2, 146–150	38.26	*Idmidronea* spp.	1.24	1.39	0.0	100.0	4.9	1.24	1.09
5H-3, 40–42	38.70	*Idmidronea* spp.	1.25	1.41	0.0	100.0	4.3	1.25	1.15
5H-5, 40–42	41.70	*Idmidronea* spp.	1.43	1.87	0.0	100.0	4.0	1.43	1.63
5H-5, 66–70	41.96	*Idmidronea* spp.	1.08	1.97	0.0	100.0	3.3	1.08	1.77
6H-1, 41–43	45.21	*Idmidronea* spp.	1.69	2.08	0.0	100.0	3.9	1.69	1.85
6H-2, 87–91	47.17	*Idmidronea* spp.	1.67	2.28	0.0	100.0	2.7	1.67	2.12
6H-3, 40–42	48.20	*Idmidronea* spp.	1.19	2.05	0.0	100.0	7.6	1.19	1.59
6H-4, 130–134	50.60	*Idmidronea* spp.	1.39	2.03	0.0	100.0	4.6	1.39	1.76
6H-5, 40–42	51.20	*Idmidronea* spp.	1.13	2.03	0.0	100.0	4.4	1.13	1.77
7H-2, 67–71	56.47	*Idmidronea* spp.	0.91	1.81	0.0	100.0	6.1	0.91	1.44
7H-3, 40–42	57.70	*Idmidronea* spp.	0.92	1.65	0.0	100.0	5.5	0.92	1.32
7H-5, 40–42	60.70	*Idmidronea* spp.	0.77	1.68	0.0	100.0	5.6	0.77	1.35
8H-5, 40–42	70.20	*Idmidronea* spp.	0.77	1.98	0.0	100.0	5.3	0.77	1.66

Table T1 (continued).

Core, section, interval (cm)	Depth (mbsf)	Bryozoan species	δ¹³C (‰ VPDB)	δ¹⁸O (‰ VPDB)	Aragonite (wt%)	Calcite (wt%)	Mg (mol%)	δ¹³C_corr (‰ VPDB)	δ¹⁸O_corr (‰ VPDB)
					Mineralogy				
8H-6, 68–72	71.98	*Idmidronea* spp.	0.78	1.97	0.0	100.0	4.7	0.78	1.69
9H-3, 40–42	76.70	*Idmidronea* spp.	0.74	2.10	0.0	100.0	3.6	0.74	1.89
9H-3, 105–109	77.35	*Idmidronea* spp.	0.81	2.14	0.0	100.0	3.9	0.81	1.91
9H-5, 40–42	79.70	*Idmidronea* spp.	1.41	1.62	0.0	100.0	NA	1.41	(1.62)
10H-2, 139–143	85.69	*Idmidronea* spp.	0.73	2.02	0.0	100.0	4.2	0.73	1.77
10H-3, 40–42	86.20	*Idmidronea* spp.	0.68	2.08	0.0	100.0	4.3	0.68	1.82
10H-5, 40–42	89.20	*Idmidronea* spp.	0.96	1.96	0.0	100.0	3.8	0.96	1.74
11H-3, 40–42	95.70	*Idmidronea* spp.	1.11	2.01	0.0	100.0	5.0	1.11	1.71
11H-5, 13–17	98.43	*Idmidronea* spp.	0.92	1.98	0.0	100.0	5.3	0.92	1.67
11H-5, 40–42	98.70	*Idmidronea* spp.	0.86	2.06	0.0	100.0	3.6	0.86	1.84
12H-5, 143–147	109.23	*Idmidronea* spp.	0.80	2.11	0.0	100.0	5.9	0.80	1.75
13H-2, 129–133	114.09	*Idmidronea* spp.	1.00	2.16	0.0	100.0	4.7	1.00	1.88
13H-2, 129–133	114.09	*Idmidronea* spp.	0.93	2.32	0.0	100.0	5.3	0.93	2.00
13H-2, 129–133	114.09	*Idmidronea* spp.	0.85	2.22	0.0	100.0	5.3	0.85	1.90
13H-4, 130–134	117.10	*Idmidronea* spp.	1.57	2.01	0.0	100.0	6.4	1.57	1.62
14H-3, 115–119	124.95	*Idmidronea* spp.	1.09	1.67	0.0	100.0	5.3	1.09	1.36
182-1132B-									
1H-2, 123–127	2.73	*Nevianipora* sp.	1.48	1.98	0.0	100.0	3.8	1.48	1.75
1H-3, 07–11	3.07	*Nevianipora* sp.	1.25	1.85	0.0	100.0	4.3	1.25	1.59
1H-3, 40–42	3.40	*Nevianipora* sp.	1.58	1.80	0.0	100.0	2.9	1.58	1.63
1H-5, 50–54	6.50	*Nevianipora* sp.	1.33	1.87	0.0	100.0	2.7	1.33	1.71
2H-1, 146–150	8.26	*Nevianipora* sp.	1.40	1.84	0.0	100.0	1.5	1.40	1.75
2H-2, 76–80	9.06	*Nevianipora* sp.	1.75	1.90	0.0	100.0	2.6	1.75	1.74
2H-3, 04–8	9.84	*Nevianipora* sp.	1.11	1.61	0.0	100.0	3.4	1.11	1.41
2H-3, 04–8	9.84	*Nevianipora* sp.	1.31	2.05	0.0	100.0	2.6	1.31	1.89
2H-3, 04–8	9.84	*Nevianipora* sp.	1.42	1.86	0.0	100.0	2.4	1.42	1.72
2H-3, 04–8	9.84	*Nevianipora* sp.	1.17	1.47	0.0	100.0	4.0	1.17	1.23
2H-3, 04–8	9.84	*Nevianipora* sp.	1.49	1.84	0.0	100.0	3.7	1.49	1.62
2H-3, 04–8	9.84	*Nevianipora* sp.	1.33	1.71	0.0	100.0	3.9	1.33	1.48
2H-3, 04–8	9.84	*Nevianipora* sp.	1.44	1.64	0.0	100.0	2.3	1.44	1.50
2H-3, 40–42	10.20	*Nevianipora* sp.	1.00	1.62	0.0	100.0	2.5	1.00	1.47
2H-4, 72–76	12.02	*Nevianipora* sp.	1.36	1.54	0.0	100.0	3.1	1.36	1.35
2H-5, 40–42	13.20	*Nevianipora* sp.	1.03	1.53	0.0	100.0	3.5	1.03	1.33
2H-5, 81–85	13.61	*Nevianipora* sp.	1.03	1.52	0.0	100.0	2.6	1.03	1.37
2H-6, 96–100	15.26	*Nevianipora* sp.	1.12	1.47	0.0	100.0	2.0	1.12	1.34
2H-CC, 05–7	16.12	*Nevianipora* sp.	1.14	1.55	0.0	100.0	2.1	1.14	1.42
3H-2, 146–150	19.26	*Nevianipora* sp.	1.11	1.51	0.0	100.0	3.8	1.11	1.28
3H-3, 40–42	19.70	*Nevianipora* sp.	1.14	1.48	0.0	100.0	2.2	1.14	1.35
3H-3, 130–134	20.60	*Nevianipora* sp.	1.11	1.49	0.0	100.0	3.5	1.11	1.28
3H-4, 72–76	21.52	*Nevianipora* sp.	1.22	1.34	0.0	100.0	2.4	1.22	1.19
3H-5, 40–42	22.70	*Nevianipora* sp.	1.00	1.44	0.0	100.0	2.8	1.00	1.27
3H-5, 123–125	23.53	*Nevianipora* sp.	1.21	1.40	0.0	100.0	2.8	1.21	1.23
4H-1, 146–150	27.26	*Nevianipora* sp.	1.20	1.61	0.0	100.0	3.2	1.20	1.42
4H-3, 40–42	29.20	*Nevianipora* sp.	1.13	1.78	0.0	100.0	2.5	1.13	1.63
4H-4, 01–3	30.31	*Nevianipora* sp.	0.85	1.59	0.0	100.0	3.1	0.85	1.41
4H-4, 89–93	31.19	*Nevianipora* sp.	1.27	1.64	0.0	100.0	2.2	1.27	1.50
4H-5, 40–42	32.20	*Nevianipora* sp.	1.19	1.70	0.0	100.0	1.8	1.19	1.59
4H-5, 142–144	33.22	*Nevianipora* sp.	1.15	1.54	0.0	100.0	4.7	1.15	1.26
4H-6, 46–50	33.76	*Nevianipora* sp.	0.70	1.27	0.0	100.0	2.5	0.70	1.11
4H-7, 50–54	34.80	*Nevianipora* sp.	0.83	1.24	0.0	100.0	2.5	0.83	1.09
5H-2, 146–150	38.26	*Nevianipora* sp.	0.98	1.28	0.0	100.0	2.7	0.98	1.12
5H-3, 40–42	38.70	*Nevianipora* sp.	0.77	1.17	0.0	100.0	2.6	0.77	1.01
5H-5, 40–42	41.70	*Nevianipora* sp.	0.57	1.69	0.0	100.0	2.4	0.57	1.55
5H-5, 66–70	41.96	*Nevianipora* sp.	0.83	1.88	0.0	100.0	3.8	0.83	1.65
5H-6, 75–79	43.55	*Nevianipora* sp.	0.88	1.92	0.0	100.0	3.4	0.88	1.72
6H-1, 41–43	45.21	*Nevianipora* sp.	1.15	2.17	0.0	100.0	2.7	1.15	2.01
6H-2, 87–91	47.17	*Nevianipora* sp.	0.84	2.13	0.0	100.0	1.1	0.84	2.07
6H-3, 40–42	48.20	*Nevianipora* sp.	1.13	2.13	0.0	100.0	3.5	1.13	1.91
6H-4, 130–134	50.60	*Nevianipora* sp.	0.80	2.02	0.0	100.0	3.4	0.80	1.82
6H-5, 40–42	51.20	*Nevianipora* sp.	0.62	1.91	0.0	100.0	3.0	0.62	1.73
7H-2, 67–71	56.47	*Nevianipora* sp.	0.68	1.68	0.0	100.0	3.3	0.68	1.48
7H-3, 40–42	57.70	*Nevianipora* sp.	0.37	1.66	0.0	100.0	2.7	0.37	1.50
7H-5, 40–42	60.70	*Nevianipora* sp.	0.41	1.57	0.0	100.0	2.7	0.41	1.41
8H-3, 40–42	67.20	*Nevianipora* sp.	0.35	1.57	0.0	100.0	2.9	0.35	1.40
8H-5, 40–42	70.20	*Nevianipora* sp.	0.60	1.96	0.0	100.0	1.6	0.60	1.86
8H-6, 68–72	71.98	*Nevianipora* sp.	0.36	1.85	0.0	100.0	5.8	0.36	1.50
9H-3, 40–42	76.70	*Nevianipora* sp.	0.39	1.95	0.0	100.0	5.7	0.39	1.60
9H-3, 105–109	77.35	*Nevianipora* sp.	0.60	2.06	0.0	100.0	2.8	0.60	1.90

Table T1 (continued).

| Core, section, interval (cm) | Depth (mbsf) | Bryozoan species | $\delta^{13}C$ (‰ VPDB) | $\delta^{18}O$ (‰ VPDB) | Mineralogy | | | $\delta^{13}C_{corr}$ (‰ VPDB) | $\delta^{18}O_{corr}$ (‰ VPDB) |
					Aragonite (wt%)	Calcite (wt%)	Mg (mol%)		
9H-5, 40–42	79.70	*Nevianipora* sp.	1.10	1.82	0.0	100.0	2.9	1.10	1.64
10H-2, 139–143	85.69	*Nevianipora* sp.	0.51	1.95	0.0	100.0	5.5	0.51	1.62
10H-3, 40–42	86.20	*Nevianipora* sp.	0.33	1.92	0.0	100.0	4.8	0.33	1.63
10H-5, 40–42	89.20	*Nevianipora* sp.	0.62	1.81	0.0	100.0	3.5	0.62	1.60
11H-3, 40–42	95.70	*Nevianipora* sp.	0.45	2.06	0.0	100.0	4.7	0.45	1.78
11H-5, 40–42	98.70	*Nevianipora* sp.	0.79	2.09	0.0	100.0	NA	0.79	(2.09)
12H-5, 143–147	109.23	*Nevianipora* sp.	0.55	2.18	0.0	100.0	5.5	0.45	1.85
13H-2, 129–133	114.09	*Nevianipora* sp.	0.81	2.11	0.0	100.0	6.0	0.81	1.75
13H-2, 129–133	114.09	*Nevianipora* sp.	1.05	2.24	0.0	100.0	5.1	1.05	1.94
13H-4, 130–134	117.10	*Nevianipora* sp.	0.92	1.82	0.0	100.0	3.9	0.92	1.59
14H-3, 115–119	124.95	*Nevianipora* sp.	0.70	1.81	0.0	100.0	4.7	0.70	1.52

Notes: NA = samples not enough for XRD measurements. $\delta^{13}C_{corr}$ = carbon isotopic value corrected to pure calcite; $\delta^{18}O_{corr}$ = oxygen isotopic value corrected to pure calcite.